UNIVERSITY OF MINNESOTA
ST. ANTHONY FALLS LABORATORY
Engineering, Environmental and Geophysical Fluid Dynamics

Project Report No. 526

MINUHET (Minnesota Urban Heat Export Tool): A software tool for the analysis of stream thermal loading by urban stormwater runoff

by

William Herb, Ben Janke, Omid Mohseni and Heinz Stefan

Prepared for

Minnesota Pollution Control Agency
St. Paul, Minnesota

March 2009
Minneapolis, Minnesota

Abstract

Urbanization affects the temperature of cold water resources, coldwater streams in particular. In Minnesota such streams are typically found in well-shaded watersheds and receive large groundwater inputs. They are ecologically significant because they support coldwater fisheries and other wildlife that would be unable to survive in warmer streams. The conversion of land from existing agricultural use or natural conditions poses a threat to these streams. Urban expansion usually requires removing crops and trees and replacing them with buildings, parking lots, roads, lawns, and parks. These changes affect shading, heat transfer, and hydrology within the watershed. Currently, there are few tools available to project to what extent stream temperatures are influenced by development in the watershed.

This report describes a new simulation tool, MINUHET (Minnesota Urban Heat Export Tool). MINUHET is a tool used to simulate the flow of stormwater surface runoff and its associated heat content through a small watershed for one or several rainfall event of interest. The tool includes hydrologic and thermal models for surface runoff, natural and man-made drainage networks, and stormwater treatment ponds. The main output of MINUHET is a time series of flow rates and temperatures at the outlet of the watershed, to enable prediction of thermal impact on receiving streams. MINUHET is event-based, i.e. it is designed primarily to simulate a single storm event. The MINUHET tool includes a database of observed and/or synthetic storm events that have the potential to produce high thermal loading in receiving streams.

Verification of MINUHET has been performed at both the component level and the system level. The surface temperature model was verified for a number of different impervious and pervious land surfaces for continuous, multi-month simulations of wet and dry conditions. The runoff model has been compared to other models, including a more complex kinematic wave model and a commercial runoff model (EPA-SWMM), and to observed runoff time series from a parking lot. The pond model component was used successfully to simulate several months of observed water level and temperature data for a wet detention pond in Woodbury, MN. The MINUHET tool has been applied to a 12 acre residential development in Plymouth, MN that was instrumented in 2005.

A common application of MINUHET may be to compare the thermal loading of stormwater runoff from an area of land before and after development, to quantify possible increases in thermal loading due to development. MINUHET includes components for developed and undeveloped land parcels (sub-watersheds), pervious and impervious open channels, storm sewer systems, and stormwater ponds. MINUHET does not include a stream temperature model, so that while MINUHET can be used to simulate the heat loading to a stream, it cannot be used, by itself, to simulate the resulting change in stream temperature.

Table of Contents

1. Introduction

1.1 Model Concept

Urbanization affects the temperature of cold water resources, streams in particular. Cold-water streams in Minnesota typically exist in well-shaded watersheds and have large water inputs from groundwater. They are ecologically significant because they support coldwater fisheries and other wildlife that would be unable to survive in warmer streams. The conversion of land from existing agricultural use or natural conditions can pose a threat to a coldwater stream. Urban expansion usually requires removing crops and trees and replacing them with buildings, parking lots, roads, lawns, and parks. These changes affect shading, heat transfer, and hydrology within the watershed. Currently, there are few tools available to project to what extent stream temperatures are influenced by development in the watershed.

This report describes a new simulation tool, MINUHET (Minnesota Urban Heat Export Tool). MINUHET is a tool used to simulate the flow of stormwater surface runoff and its associated heat content through a small watershed for one or several rainfall events of interest. The main output of MINUHET is a time series of flow rates and temperatures at the outlet of the watershed, to enable prediction of thermal impact on receiving streams. MINUHET is event-based, i.e. it is designed primarily to simulate a single storm event. The MINUHET tool includes a database of observed and/or synthetic storm events that have the potential to produce high thermal loading in receiving streams.

The overall process of assembling and running a model within MINUHET is depicted in Figure 1.1. MINUHET requires the input of basic descriptions of sub-watersheds (pervious and impervious areas, slopes, etc.), drainage network elements (lengths, diameters, slopes, etc.) and ponds (bathymetry, output structures, etc.). The connectivity of the individual components is established by constructing a drainage schematic of the watershed. MINUHET is not capable of directly importing spatial information from, e.g., GIS shape files, but GIS software is helpful for preparing the needed parameters for the model components. The drainage network can include mitigation ponds, including wet ponds, dry ponds, infiltration pods, and rain gardens. Storm events to apply to the model are selected based on one of seven climate regions within Minnesota.

A common application of MINUHET may be to compare the thermal loading of stormwater runoff from an area of land before and after development, to quantify possible increases in thermal loading due to development (Herb 2008a). As a result, MINUHET includes components for developed and undeveloped land parcels (sub-watersheds), pervious and impervious open channels, storm sewer systems, and stormwater ponds. MINUHET does not include a stream temperature model, so that while MINUHET can be used to simulate the heat loading to a stream, it cannot be used, by itself, to simulate the resulting change in stream temperature.

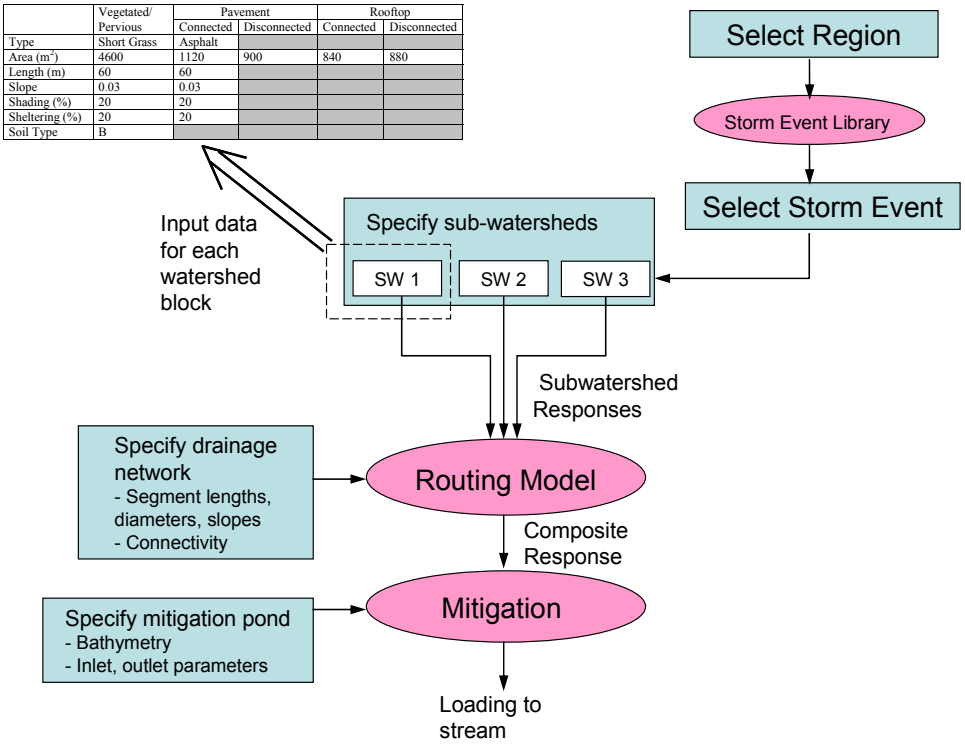

Figure 1.1. Schematic diagram of the process of assembling and running an MINUHET model.

1.2 Model Structure

MINUHET is a self-contained software tool that includes several model component executables and a graphical user interface (Figure 1.2). There are three main sub-programs that perform the runoff and heat transfer calculations: the runoff model, the routing model, and the pond model. The sub-programs are written and compiled in FORTRAN 90. Although the model components could be run using MSDOS commands, a graphical user interface (GUI) was developed for the model to make it easier to design the model, enter the required watershed parameters, and to provide visualization of the system layout and simulation results. Under SAFL guidance, the GUI was developed by Minnetonka Audio Software, Inc., based on the Microsoft.NET framework.

Each of the three main FORTRAN model components must calculate a balance for the surface runoff flow rate (Q) and for the heat flux (H) contained in the surface runoff, as shown schematically in Figure 1.3. By definition, sub-watersheds receive precipitation but not surface inflow (Q_{in}= 0). Drainage network components and stormwater ponds may add or subtract flow and heat content, depending on the particular watershed and storm event.

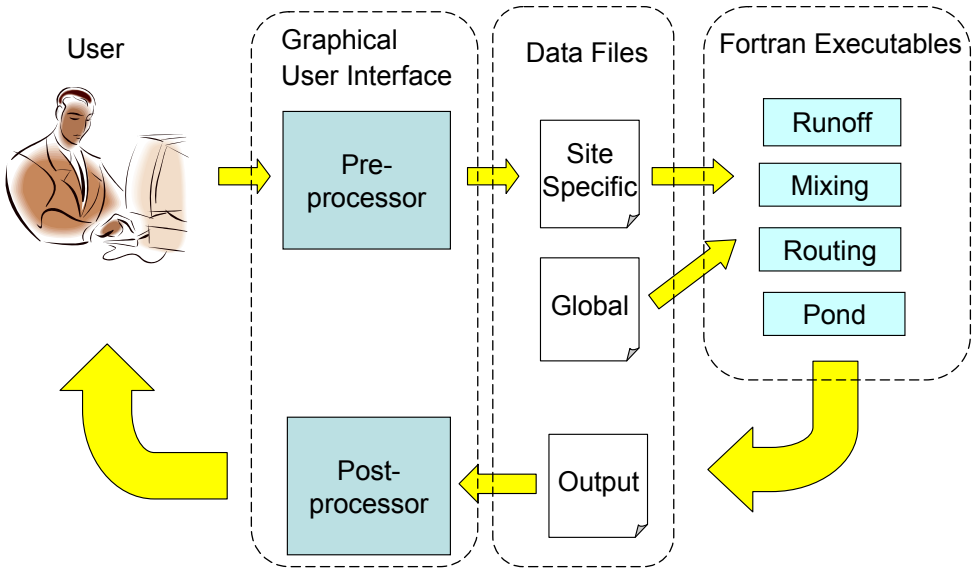

Figure 1.2. The structure of MINUHET

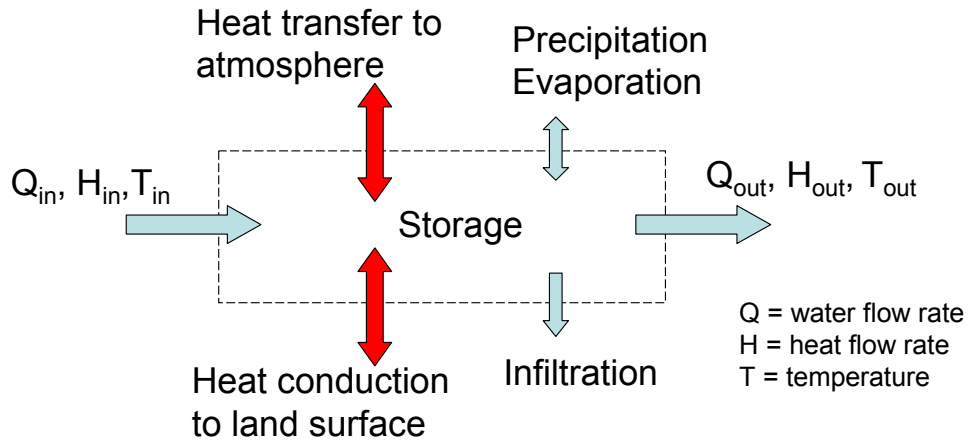

Figure 1.3. Schematic diagram for the balance of runoff flow and heat flux for each sub-watershed, drainage network, and pond component.

The MINUHET sub-watershed model has two major components: 1) a land surface temperature model, 2) a surface runoff model. The land surface temperature model is based on a surface heat transfer model that calculates the radiation, convection, and evaporation components based on specified climate. A one-dimensional finite difference model is then used to calculate the vertical conduction of heat through the soil column and the soil temperature profile to a depth of one meter. The MINUHET storm files include at least several days of antecedent climate conditions prior to the rainfall event, so that realistic surface temperatures and soil temperature

profiles are calculated before the rainfall event begins. During a rainfall event, the surface temperature model calculates the heat transfer between the surface runoff and the land surface, such that the surface runoff and the land surface reach the same temperature. Details of the surface temperature model are given in Section 2.1, Appendix A, Herb et al. 2006a, and Herb et al. 2008b.

The surface runoff model was created to simulate runoff from relatively small impervious areas, e.g. a parking lot, at high time resolution, for steady or unsteady rainfall events. The runoff model uses an analytic formulation to simulate the time history of flow rate and temperature at the outlet of an area with uniform slope. The analytic model is based on Manning's equation, and closely matches the results of a kinematic wave model. The runoff model is described in more detail in Section 2.1, Appendix C, and in SAFL Project Report #484 (Herb et al. 2006c).

The hydro-thermal routing model uses a kinematic wave algorithm to simulate the flow of water and heat through a drainage network. In its current configuration, the routing model does not include atmospheric heat transfer for the routing elements, so that it is not appropriate to simulate long open channel drainage networks. The routing model does not include junction losses, so that MINUHET should not be used as a tool for designing stormwater handling systems. There are three types of routing elements available for simulation of a drainage network: circular storm sewer pipes, impervious open channels (e.g. concrete open channels) with trapezoidal cross section, and pervious open channels with trapezoidal cross section. Infiltration and heat transfer to the channel/pipe wall is included where appropriate.

The MINUHET pond model can be used to simulate wet detention ponds, infiltration ponds and rain gardens, and dry ponds. The pond model is based on previous 1-D models for lakes (Ford and Stefan 1980, Hondzo and Stefan 1993) and wastewater detention ponds (Gu and Stefan 1995). Given the inflow rates and temperatures of the storm sewers discharging to a pond, the hydrology of the inflows, and the design of any outlet structure, the model projects the rate and temperature of the outflow from the pond. The pond vertical temperature profile is calculated for each time step based on atmospheric heat transfer, heat conduction through the pond bottom, and the flow rate and temperature of inflows. Atmospheric heat transfer includes solar and long wave radiation components, atmospheric convection, and evaporation. Pond level is calculated based on inflow and outflow rates, infiltration, direct precipitation, and evaporation. Further details on the MINUHET pond model may be found in Section 2.3 and SAFL Technical Report #479 (Herb et al 2006b).

2. The MINUHET Model Components

MINUHET includes three major model components: a sub-watershed model that simulates runoff and runoff temperature for areas of uniform or mixed land use, a routing model that routes flow and heat through natural or man-made drainage networks, and a pond model that performs hydrothermal simulation of wet ponds, infiltration basins, dry ponds, and rain gardens.

2.1 The Sub-watershed Model

The sub-watershed model includes a land surface temperature model that establishes surface temperatures prior to and during rainfall events, a semi-analytic runoff model that simulates runoff rate from land surfaces at one minute time steps, and a model for the thermal coupling of land surfaces and runoff that determines the runoff temperature. The sub-watershed model is discussed in detail in SAFL report #484 (Herb et al. 2006c).

Land surface temperature model
The land surface temperature model is based on a surface heat transfer model that calculates the radiation, convection, and evaporation components based on specified climate (Figure 2.1.1). The net surface heat flux is calculated as a function of time for unvegetated surfaces based on net radiation (h_{rad}), evaporation (h_{evap}), convection (h_{conv}), and runoff heat transfer (h_{ro}):

$$h_{net} = h_{rad} - h_{evap} - h_{conv} - h_{ro} \tag{2.1.1}$$

For paved surfaces, the evaporative and runoff heat fluxes are set to zero except during rainfall events and after rainfall events when standing water is present. The complete set of equations used to calculate the surface heat transfer components are given in Appendix A. For vegetated surfaces, a more complex surface heat transfer formulation is used that includes a separate heat balance equation for the plant canopy (Figure 2.1.2, Equations 2.1.2 and 2.1.3), a representative plant canopy temperature, and a distinct air temperature and humidity within the canopy. The plant canopy is assumed to have negligible thermal mass, so that the heat balance given in Equation 2.2 is maintained at all times, e.g. heat storage is zero.

$$h_{rad,a} - h_{rad,g} - h_{evap,f} - h_{conv,f} = 0 \tag{2.1.2}$$

$$h_{net,g} = h_{rad,net,g} - h_{evap,g} - h_{conv,g} - h_{ro} \tag{2.1.3}$$

where $h_{rad,a}$, $h_{rad,g}$, $h_{rad,f}$, and $h_{conv,f}$ are the atmospheric radiation, ground radiation, evaporation, and convection heat fluxes to the plant canopy, respectively; $h_{net,g}$ is the net heat flux to the ground surface, and $h_{rad,net,g}$, $h_{evap,g}$ and $h_{conv,g}$ are the radiation, evaporation, and convection heat fluxes to the ground surface. The complete set of equations used for to calculate surface heat transfer, including the effects of a plant canopy, is given in Appendix B.

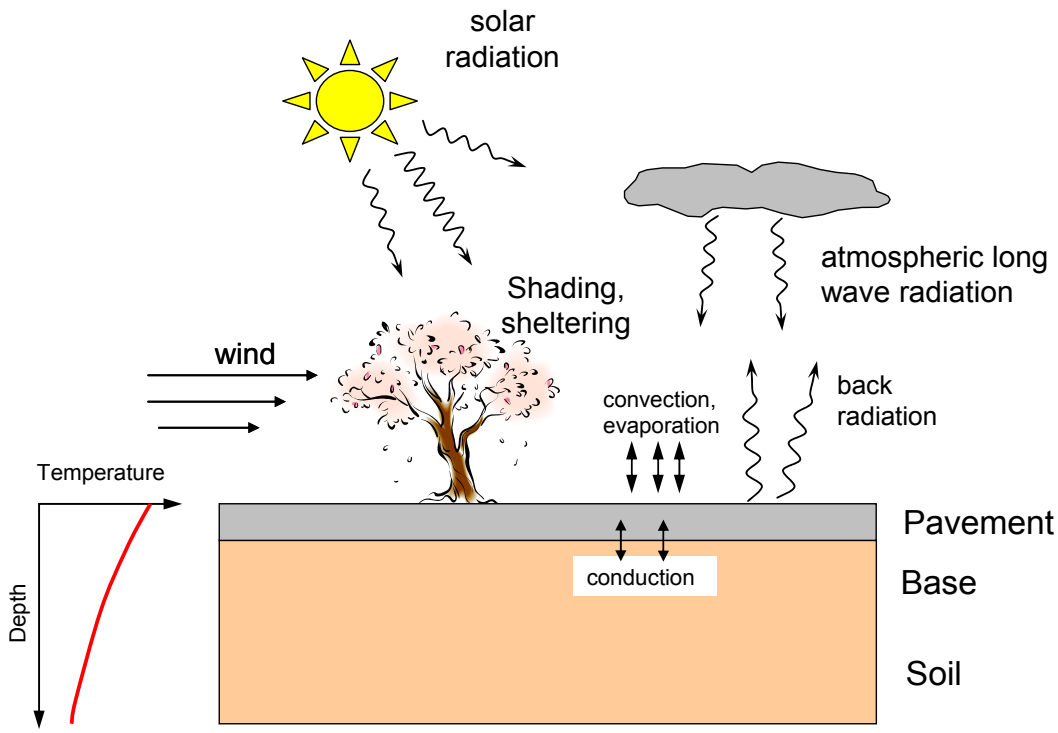

Figure 2.1.1 Processes included in the MINUHET surface temperature model.

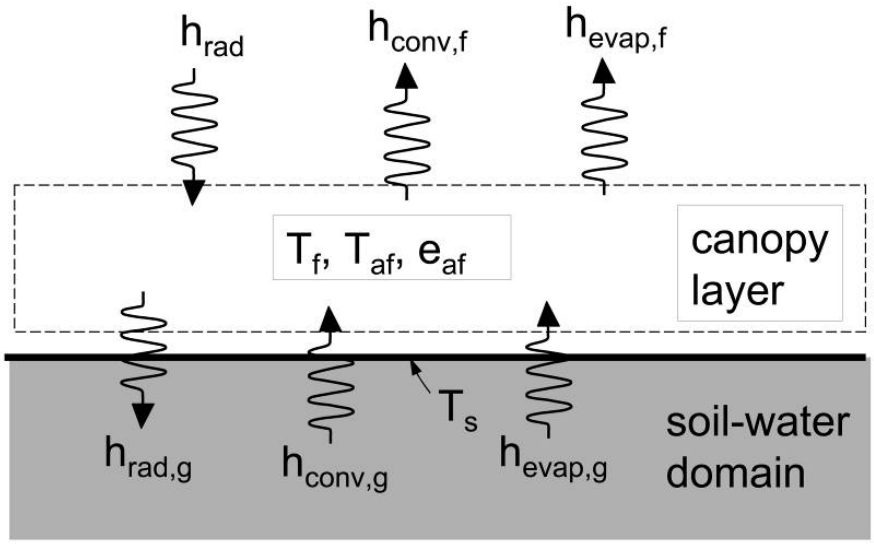

Figure 2.1.2. Ground surface heat transfer components with a plant canopy.

Soil temperature model

A one-dimensional finite-difference model is used to calculate the vertical conduction of heat through the soil column and the soil temperature profile to a depth of one meter, based on an equation for unsteady diffusion and storage of heat (Equation 2.1.4). The heat conduction equation is solved using finite difference formulations, as detailed in Appendix C. Additional information and results are given by Herb et al. 2006a.

$$\frac{\partial T}{\partial t} = \frac{\partial}{\partial z}\left(D \frac{\partial T}{\partial z} \right) \tag{2.1.4}$$

where T is soil temperature as a function of depth (z), and D is the thermal diffusivity of the soil. A recently added feature of MINUHET is that the soil thermal diffusivity (D), and density-specific heat product (ρC_p) are adjusted based on water content, using linear fits of observed relationships of diffusivity and specific heat to volume fraction air given by Ochsner et al. (2001):

$$D(\theta) = D_{sat}\left(1 - 1.43\left(\theta_{sat} - \theta\right)\right) \tag{2.1.5}$$

$$\rho C_p(\theta) = \left(\rho C_p\right)_{sat}\left(1 - \left(\theta_{sat} - \theta\right)\right) \tag{2.1.6}$$

where θ is the fractional soil moisture content and θ_{sat}, D_{sat}, and $(\rho C_p)_{sat}$ are the saturated soil moisture content, thermal diffusivity, and density-specific heat product, respectively. The surface heat transfer for vegetated (Equations 2.1.2, 2.1.3) or bare (Equation 2.1.1) surfaces is used as the upper boundary condition, while a fixed temperature is specified for the lower boundary condition. The combination of a 1 m depth for the soil temperature model combined with the fixed temperature lower boundary condition limits the application of the soil temperature model to periods of a week or two. This is consistent with the intended application of MINUHET to individual rainfall events, and differs from the soil temperature models described, e.g., by Herb et al. 2006a, which use a 10 m deep soil column, and can be used to simulate soil temperature for periods of six months or more.

Roof temperature model

While typical residential roofs with asphalt shingles have little thermal mass, and therefore, little ability to influence the temperature of surface runoff, tar/gravel commercial roofs, residential tile roofs have significant thermal mass. As a result, a roof temperature model was developed and calibrated. The model has the following components:

1) The roof is represented as a thermal mass per unit area, which is a composite of the various roof layers.
2) Surface heat transfer with the atmosphere is applied as the loading, using an identical formulation to the pavement temperature model described in Appendix A. Heat transfer between the underside of the roof and the building (e.g. the attic) is assumed to be negligible.
3) Heat transfer between the roof surface and rainfall runoff is modeled using the same formulation as given in Appendix A, except that the thermal boundary layer thickness in the roof

is limited by the roof thickness, e.g. 1 cm. The differential equation for the unsteady roof temperature as a function of atmospheric heat transfer is given by:

$$\frac{dT}{dt} = \frac{h_a}{\rho C_p m'} \tag{2.1.7}$$

where m' is the roof mass per unit area, ρ and C_p are the composite density and specific heat of the roof materials, respectively, and h_a is the surface heat transfer (W/m^2). Equation 2.1.7 is discretized to the form of Equation 2.1.8:

$$T(t+\Delta t) = \frac{T(t)\left(1+\frac{\partial h}{\partial T}\frac{\Delta t}{m'C_p}\right) + h_a\frac{\Delta t}{m'C_p}}{\left(1+\frac{\partial h}{\partial T}\frac{\Delta t}{m'C_p}\right)} \tag{2.1.8}$$

where dh/dT is the surface heat transfer temperature derivative. h and dh/dT are calculated using the roof temperature from the previous time step. The temperature derivative term helps take into account the variation of heat transfer with surface temperature over the time step and makes the solution more stable.

Surface runoff model

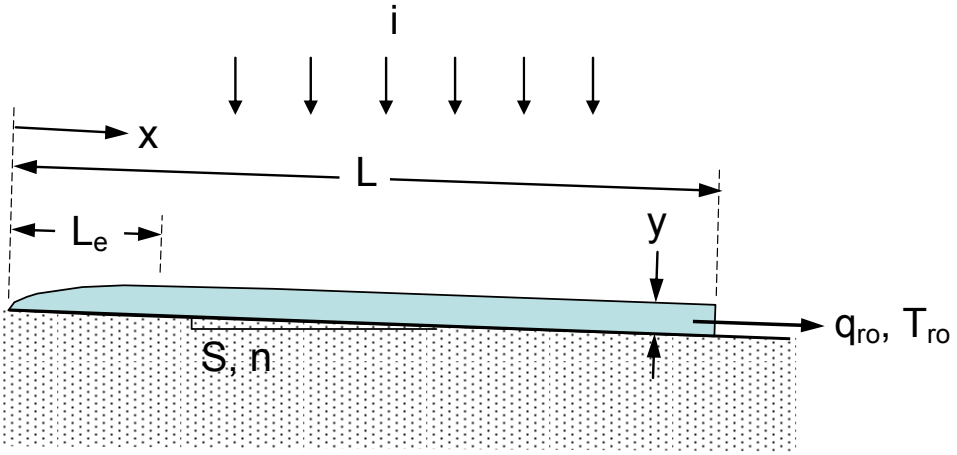

Figure 2.1.3. Schematic diagram of the parameters used in the MINUHET runoff model.

The surface runoff model was created for MINUHET to simulate runoff from relatively small impervious areas, e.g. a parking lot, at high time resolution, for steady or unsteady rainfall events. The runoff model uses a semi-analytic formulation to simulate the time history of flow rate and temperature at the outlet of an area with uniform slope (Figure 2.1.3). The runoff model is based on Manning's equations, a commonly used empirical equation relating flow rate and depth to slope and roughness for open-channel and surface runoff flows (Mays 2001).

$$q = \frac{S^{1/2} y^{2/3}}{n} \tag{2.1.9}$$

where q is the flow rate per unit width, S is slope, y is the flow depth, and n is Manning's roughness coefficient. The total length of the runoff area (L) is divided into a length, L_e, that has fully developed (equilibrium) runoff flow and the developing flow length ($L-L_e$), where the runoff thickness is assumed constant. The length of the equilibrium flow region varies as a function of time based on previously developed expressions for the time to equilibrium (t_e) (Mays, 2001).

$$t_e = \frac{n L}{S^{1/2} y^{2/3}} \tag{2.1.10}$$

Based on the defined geometry, the total runoff volume per unit width (v) is given by:

$$v = \frac{5}{8} h L_c + y\left(L - L_e\right) = y\left(L - \frac{3}{8} L_e\right) \tag{2.1.11}$$

Based on conservation of mass, the rate of change of the total runoff volume can be expressed as:

$$\frac{\partial v(t)}{\partial t} = i L - q(t) \tag{2.1.12}$$

where i is the precipitation rate. The MINUHET runoff model uses these basic equations to calculate the runoff rate and average runoff thickness as a function of time, as detailed in Appendix C.

Runoff heat transfer

An important component of the runoff model is the algorithm to calculate the heat transfer from the runoff to the land surface, as this has a major influence on the runoff temperature. The MINUHET model calculates the heat transfer between the ground surface and the runoff using the assumption that the thin runoff layer is well mixed and at the same temperature as the ground surface. Based on a heat balance, the runoff heat transfer can then be estimated as:

$$h_{ro} = i\left(\rho c_p\right)_w \left(T_{so} - T_{dp}\right)\left(\frac{\beta}{1+\beta}\right);\ \beta = \frac{\delta\left(\rho c_p\right)_p}{2P\left(\rho c_p\right)_w} \tag{2.1.13}$$

where *i* is the precipitation rate, P is the precipitation depth, $(\rho c_p)_p$ and $(\rho c_p)_w$ are (density · specific heat) for the pavement and water, respectively, δ is the thermal boundary layer thickness in the ground, T_{so} is the surface temperature at the start of the time step, and T_{dp} is the dew point

temperature (the estimate of rainfall temperature). Further details on this formulation are given in Appendix A.

Infiltration model

MINUHET calculates infiltration into the soil for each time step during a runoff event using the Green-Ampt algorithm (Mays 2001), and thereby reduces the runoff volume. The Green-Ampt model is based on an estimate for the propagation of a wetting front through the soil column during a runoff event. The rate of infiltration (f) depends on soil properties (saturated hydraulic conductivity (K), capillary soil suction (ψ)), the initial soil moisture content, and the cumulative depth of the wetting front (F) during the event. During each runoff event, an incremental depth of infiltration is calculated based on Equation 2.1.14:

$$f = K\left(\frac{\psi \Delta\theta + F}{F}\right) \qquad (2.1.14)$$

where $\Delta\theta$ is the difference between the soil moisture content and the saturated moisture content. The solution to Equation 2.1.14 is obtained using a linearized solution form given by Li et al. (1976). The use of the Green-Ampt model implies that the volume of runoff from pervious areas will depend on the chosen soil type and initial soil moisture content.

Runoff from areas of mixed land use

For residential developments, it is typically not practical to define separate sub-watersheds for each area of pavement, rooftop, and pervious area. As a result, the MINUHET tool incorporates features to lump multiple buildings into a single subwatershed. Each sub-watershed may contain a combination of pervious and impervious surface areas: up to five areas of different land use can be specified (Figure 2.1.4):

(1) The total area of connected pavement, e.g. driveways, streets, and parking areas
(2) The total area of disconnected pavement, e.g. pavement drained into pervious areas.
(3) The total surface area of the rooftop drained into connected pavement, e.g. driveways
(4) The total surface area of the rooftop drained into pervious areas (lawns, other vegetation)
(5) The total area of the pervious land.

No attempt is made to represent the detailed shapes and location of each area within the subwatershed. The connected pavement area and the impervious area are represented as an area and a characteristic length.

Thermo-hydrographs (water flow and temperature time series) are simulated using the runoff model for each subwatershed, based on the selected storm event and the subwatershed characteristics. For each subwatershed, two separate thermo-hydrographs will be calculated for the connected impervious area and for the pervious area. The two thermo-hydrographs are then combined (mixed) to give a single flow and temperature for each subwatershed using a simple mixing FORTRAN executable (Figure 2.1.5).

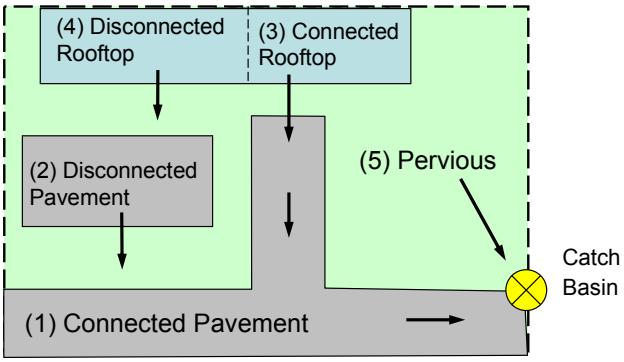

Figure 2.1.4. Schematic of developed sub-watershed, showing the five land use types and their hydraulic connectivity.

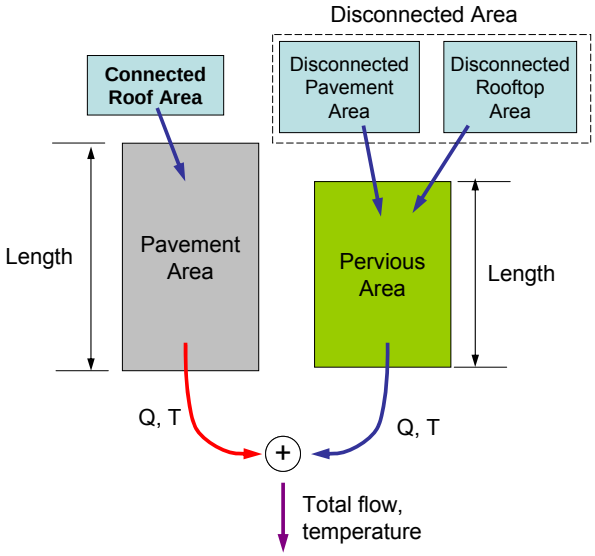

Figure 2.1.5. Flow chart of the simplified model for each sub-watershed.

2.2 The Routing Network Model

Flow Solution

The routing network model solves for the routing of flow and heat through a drainage network. The model handles natural drainage channels, e.g. small, intermittent tributaries, and constructed drainage networks, e.g. storm sewer pipes, swales, ditches, etc. In its present configuration, the MINUHET routing model calculates flow through the drainage network using a kinematic wave model. Backwater effects are not explicitly considered in the routing model, however, it is possible to consider some backwater effects by inserting pond models (Section 2.4) upstream of backwatered drainage pipe segments. Heat (water temperature) is routed through the drainage network along with flow, including the effects of wall heat transfer, e.g. heat transfer through pipe walls to the soil. The routing model does not presently include atmospheric heat transfer, thus the model should not be applied to drainage systems with long travel times (> 1 hour) through surface channels.

The flow rate through the drainage network is calculated first, using Manning's equation and a non-linear kinematic wave formulation (Chow 1976). For no lateral inflows, the equation of continuity at any point in the flow is:

$$\frac{\partial Q}{\partial x} + \frac{\partial A}{\partial t} = 0 \qquad (2.2.1)$$

where Q is the flow rate, x is the streamwise coordinate, A is the cross-sectional area of the flow, and t is time. Equation 2.2.1 has 2 unknowns, flow and area, however, flow can be related to area through Manning's equation:

$$Q = \frac{S^{1/2}}{n}\frac{A^{5/3}}{P^{2/3}} \tag{2.2.2}$$

where S is slope, n is Manning's roughness coefficient, ad P is the wetted perimeter of the flow cross-section. Combining Equations 2.2.1 and 2.1.2 produces a single, non-linear equation for flow.

$$\frac{\partial Q}{\partial x} + \alpha\beta Q^{\beta-1}\frac{\partial Q}{\partial t} = 0 \tag{2.2.3}$$

where $\alpha = \left(n\ P^{2/3}\ S^{-1/2}\right)^{0.6}$ and β=0.6. Equation 2.2.3 is discretized using a finite-difference formulation given by Chow (1976):

$$\frac{Q_{i+1,j+1} - Q_{i,j+1}}{\Delta x} + \frac{A_{i+1,j+1} - A_{i+1,j}}{\Delta t} = 0 \tag{2.2.4}$$

where i and j are the indices for distance and time, respectively, Δt is the analysis time step, and Δx is the length of the routing segment. Equation 2.2.4 is solved for each pipe or channel section, with the flow solution proceeds from upstream to downstream for each time step, calculating the flow at the downstream end of each routing segment based on the upstream value for the current and previous time steps ($Q_{i-1,j}$, $Q_{i-1,j-1}$) and the downstream value from the previous time step ($Q_{i,j-1}$). For each channel segment, an initial, linear estimate for the downstream flow is made as (Chow 1976):

$$Q_{i+1,j+1} = \frac{\frac{\Delta t}{\Delta x}Q_{i,j} + \alpha\beta Q_{i+1,j}Q_{ave}^{\beta-1}}{\frac{\Delta t}{\Delta x} + \alpha\beta Q_{ave}^{\beta-1}} \tag{2.2.5}$$

where $Q_{ave} = (Q_{i+1,j} + Q_{i,j+1})/2$. The flow determined from Equation 2.2.5 is then the initial guess for the solution to Equation 2.2.4. Newton's method is then used to iterate the solution for $Q_{i+1,j+1}$, updating the flow area A and the wetted perimeter P during each iteration. The model currently handles either circular or trapezoidal conduit cross-sections, with appropriate geometric functions to calculate P as a function of A. The flow solver assumes no backwatering effects, i.e. the pipes do not reach full capacity. For open channels, the trapezoidal cross section has no inherent depth limit. The flow solver is capable of solving for transient flow in pipes and channels, starting from a dry condition, however, a lower flow limit is established (10^{-6} m^3/s), below which flow is set to zero.

Infiltration is included in the flow calculation for pervious channels, e.g. swales. For each time step, an infiltration depth (d_i) is calculated for each channel segment, using the same Green-Ampt formulation as the surface runoff model (Equation 2.1.16). The total infiltration volume ($d_i \cdot P \cdot \Delta x$) is then subtracted from the outflow for each channel segment. A separate infiltration depth is maintained over the course of an analysis for each channel segment.

Temperature Solution

After the flow solution is completed, the temperature at each flow node in the network is calculated, beginning with the known inflow temperatures from the sub-watersheds. For each pipe or open channel, the downstream temperature is calculated using the Equation 2.2.6 based on a heat balance (Figure 2.2.1):

$$\frac{\partial}{\partial t}(V \cdot T) = Q_{in} T_{in} - Q_{out} T_{out} - H_w A_w (T - T_w) \qquad (2.2.6)$$

where T is the water temperature, V is the water volume in the pipe segment, H_w is the wall heat transfer coefficient, A_w is the wetted area in the pipe, and T_w is the temperature of the pipe wall. The wall heat transfer is calculated using the same method that is used to calculate surface runoff - land surface heat exchange (Appendix A), assuming that heat transfer is limited by conduction into the pipe wall, not by the flow boundary layer. A conductive thermal boundary layer thickness in the pipe/channel wall and surrounding soil (δ) is calculated as a function of time for each pipe or channel section, starting at the onset of a flow event. The heat transfer coefficient (H_w) is then estimated for each time step based on the boundary layer thickness as $H_w = 3K/\delta$ (Eckert and Drake 1972), where K is the thermal conductivity of the pipe wall.

Equation 2.2.6 is discretized to the following finite-difference equations:

$$\frac{(T_{i,j+1} V_{i,j+1}) - (T_{i,j} V_{i,j})}{\Delta t} = Q_{i-1,j+1} T_{i-1,j+1} - Q_{i,j+1} \overline{T}_i - \frac{3 D P \Delta x}{\delta} (\overline{T}_i - T_g) \qquad (2.2.7)$$

$$\overline{T}_i = (1 - c_{fi}) T_{i,j} + c_{fi} T_{i,j+1} \qquad (2.2.8)$$

$$c_{fi} = \frac{Q_{i,j} \Delta t}{Q_{i,j} \Delta t + V_{i,j-1}} \qquad (2.2.9)$$

where D is the thermal diffusivity of the pipe wall. The parameter c_{fi} is used to establish a weighted-average temperature $\overline{T}_i$ for the control volume over each time step that is used as the representative outflow temperature and the representative temperature for wall heat conduction. This weighting scheme was used to achieve stable temperature solutions for all flow conditions. For example, for the case of a large inflow with a small starting volume, c_{fi} approaches 1, and the inflow temperature is weighted heavily compared to the control volume temperature from the previous time step.

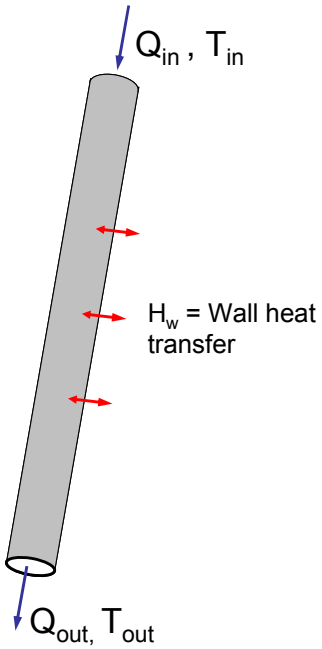

Figure 2.2.1. Schematic of the heat balance on a single pipe segment.

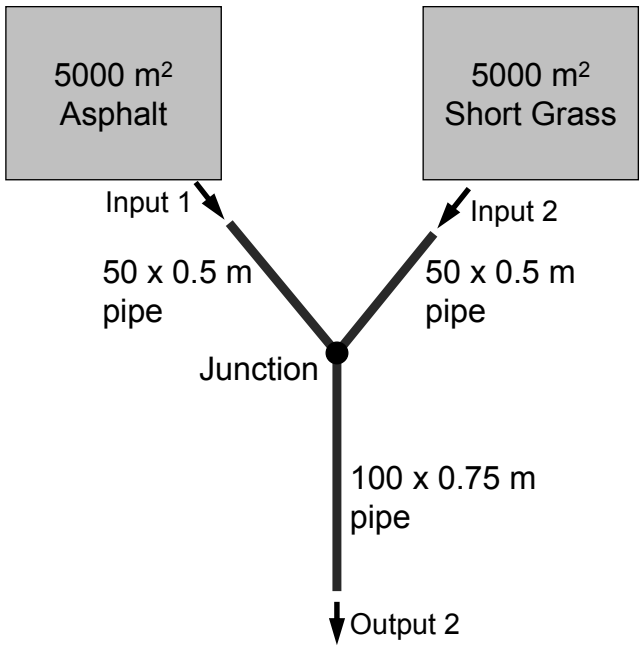

Figure 2.2.2. Schematic of example system simulated using the routing model.

As part of the pipe wall heat transfer algorithm, an initial wall temperature must be set prior to the runoff event. The pipe wall temperature is assumed to be equal to soil temperature at the burial depth. A cosine function is used to determine the seasonal variation of the soil surface temperature, and an exponential decay function is used estimate the pipe wall temperature as a function of burial depth:

$$T_g = C_0 - C_1 \, \mathrm{Exp}(-C_3) \mathrm{Cos}(2\pi(\mathrm{Cday} - C_2)/365 - C_3) \qquad (2.2.10)$$

$$C_3 = z_p \sqrt{\frac{\pi}{D\tau}} \qquad (2.2.11)$$

where Cday is the calendar day, z_p is the burial depth of the pipe, D is the thermal diffusivity, τ is the period (1 year=3.15×10^7 sec). The constants C_0, C_1, and C_2 are determined from observed or simulated seasonal soil surface temperature for the land use and climate region of interest. For the Twin Cities area and vegetated land use, C_0=10.22, C_1=12.53, and C_2=24.0, while for pavement, C_0=14.00, C_1=18.06, and C_2=15.5.

Example

An example of simulation results for the routing model is given in Figure 2.2.3 and 2.2.4. A simple system of 3 concrete pipes was created with 2 specified flow inputs (Figure 2.2.2) generated using the sub-watershed model. The flow and temperature inputs and the combined output are shown in Figure 2.2.3. The simulated flow output shows very little time delay for this system, on the order of a few minutes. The output temperature begins significantly lower than

the inflow temperatures, due to heat loss to the pipe walls. For the specified pipe burial depth in the example (2.5 m), the initial pipe wall temperature was set to 12.3 ºC. The difference in output temperature of the sewer system with and without wall heat transfer is shown in Figure 2.2.4, as well as the corresponding change in heat flow (heat export) from the system. For the relatively small rainfall event used in the example (2.9 cm), pipe wall heat transfer contributed a significant reduction in total heat export, from 1130 MJ to 750 MJ (33%).

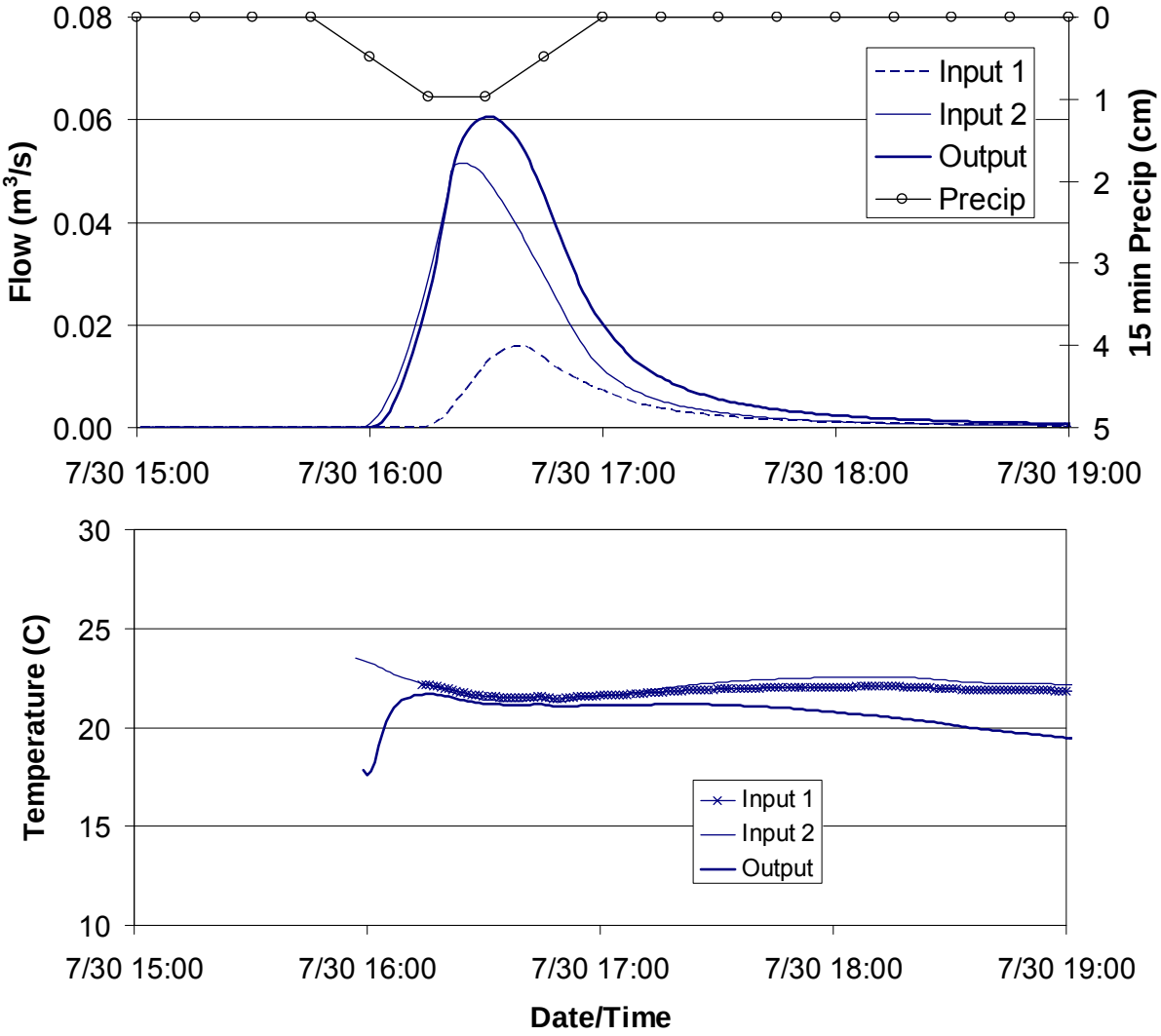

Figure 2.2.3. Simulated flow (upper panel) and temperature (lower panel) for two sub-watershed inputs (Input 1 = asphalt, Input 2 = grass) and the routing model output.

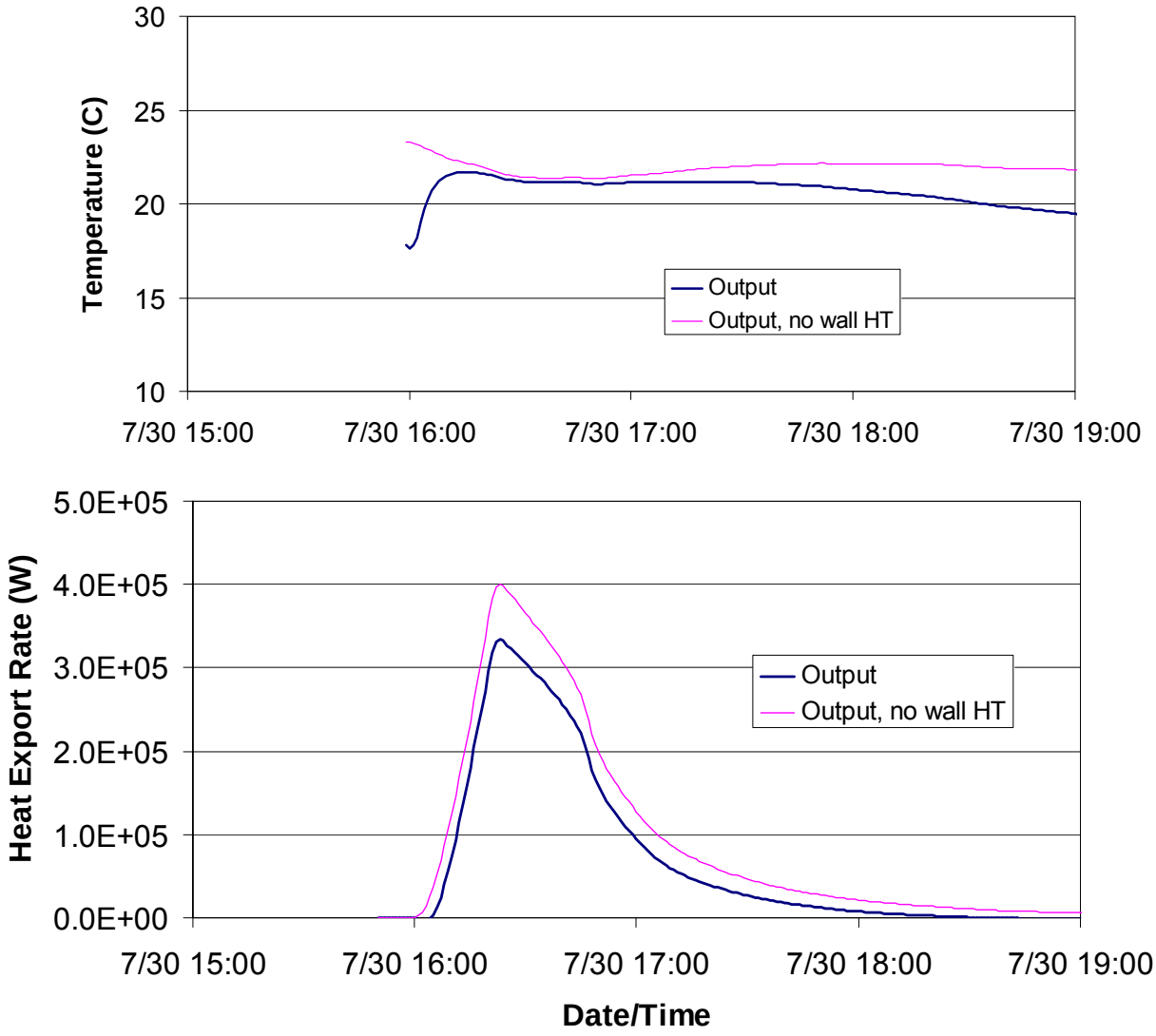

Figure 2.2.4. Simulated outflow heat export (lower panel) and temperature (upper panel) using routing model with and without pipe wall heat transfer. Pipe wall heat transfer reduced the total heat export for the event from 1130 MJ to 750 MJ.

2.3 The MINUHET Pond Model

The MINUHET pond model can be used to simulate wet detention ponds, infiltration ponds and rain gardens, and dry ponds. The purpose of the pond model is to simulate the pond response (outflow rate and temperature) to stormwater inflow events. The outflow rate and temperature depend on both the initial condition of the pond prior to the event (stage, temperature) and the characteristics of the inflow event. The processes considered in the MINUHET pond model are

illustrated in Figure 2.3.1. Further information and details on the MINUHET pond model may be found in SAFL Project Report #479 (Herb et al 2006b).

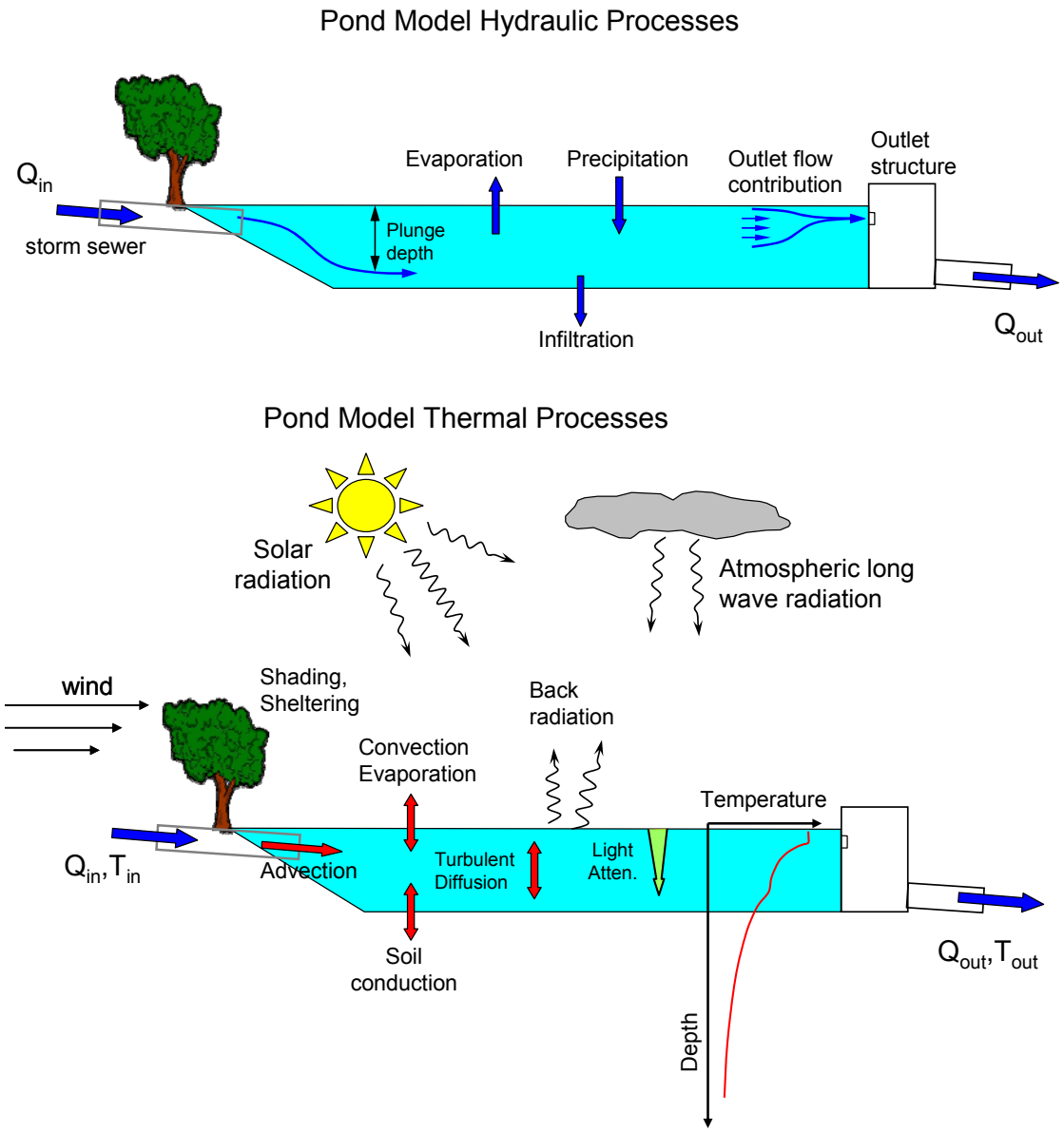

Figure 2.3.1. Schematic of hydraulic (top) and thermal (bottom) processes in the pond model

Similar to previous 1-D models of lakes (Ford and Stefan 1980, Hondzo and Stefan 1993) and wastewater detention ponds (Gu and Stefan 1995) the model divides a stormwater detention pond into a system of horizontal water layers, and simulates the time-variable (hourly to daily) water temperature as well as in- and outflow rates for each layer. Given the flow rate and temperature of the inflows from storm sewers, and the design of the outlet structure, the model

projects the rate and temperature of the outflow from the pond. Pond bathymetry and weather data are required to run the model. The model uses and solves equations that describe flow and heat transfer processes in the pond, as summarized in Figure 2.3.1.

Pond Water Balance Model

The pond water volume is calculated for each time step based on inflow (Q_{in}) and outflow (Q_{out}) rates, and the precipitation (P), evaporation (d_e), and infiltration (h_i) from the pond into the ground:

$$\Delta V = (Q_{in}-Q_{out})\,\Delta t + (P-d_e-d_i)\,AT_o \qquad (2.3.1)$$

where ΔV is the change in pond volume for the time step (Δt) , AT_o is the surface area of the pond surface. Unlike the surface runoff model, infiltration through the pond bottom is specified as a fixed rate, rather than calculated using, e.g., the Green-Ampt model. From the water volume, the water depth and surface area of a pond are then calculated based on a specified area-depth relationship. The number of layers in the pond model is adjusted as the water level changes, so that the layer thickness stays within a specified range (e.g. 0.1 to 0.3m).

The specified inflows to the pond are treated as a jet-like buoyant flow. If it is denser than the pond surface, it will plunge below the pond surface until it reaches a water layer with the same density. Inflow dilution by entrainment during the plunging flow is estimated based on numerical models developed by Fang and Stefan (2000). The amount of entrainment by the inflow is estimated based on the inflow Froude number (Fr), which measures the relative magnitude of buoyancy and momentum forces in the inflow jet:

$$Q_{ent} = Q_{in}\,\frac{(0.39 + 0.22\mathrm{Fr})}{(c_f\, b/h)^{0.275}} \qquad (2.3.2)$$

where Q_{ent} is the flow rate of the inflow with entrainment, $\mathrm{Fr} = U_{in}\left(g\,\Delta\rho\,h\right)^{-1/2}$, Q_{in} and U_{in} are the inflow rate and velocity, c_f is the bottom roughness in the pond, b and h are width and depth of the inflow, $\Delta\rho$ is the difference in density between inflow and the pond water at the point of inflow. The diluted inflow is added to and mixed with the layer in the pond model which most closely matches the density of the diluted inflow.

Outflows are calculated for each time step based on the current pond level and the specified geometry of the outlet structure or structures. The pond model was developed to handle a variety of outflow structures, including circular ports, weirs, and pipes. Tailwater effects are neglected. The following equations are used for V-notch, broad-crested, and sharp-crested weirs (FHWA 1996):

V-notch weir: $Q = C_{wv}\,\mathrm{Tan}(\theta/2)\,\Delta h^{5/2}\,(2g)^{1/2}$ (2.3.3)

Broad-crested weir: $Q = C_{wb}\,\Delta h^{3/2}\,B\,(2g)^{1/2}$ (2.3.4)

Sharp-crested weir: $Q = C_{ws}\,\Delta h^{3/2}\,B\,(2g)^{1/2}$ (2.3.5)

where θ is the inside angle of the v-notch weir, in radians, C_{wv}, C_{wb}, C_{ws} are the weir coefficients for v-notch, broad-crested, and sharp-edged weirs, respectively, g is the acceleration of gravity, Δh is the distance from the pond surface above the invert of the weir, and B is the weir width. The weir coefficients are nominally set as C_{wv} = 0.31, C_{wb} = 0.38, and C_{ws} = 0.41 (FHWA 1996).

Pipe and orifice outflows are treated with a combination of weir, orifice, and pipe flow equations to handle different cases. If the pond water level is below the top of the orifice/pipe opening, a sharp-edged weir flow equation is used to calculate flow:

$$Q = C_{ws}\, A\, (2g\Delta h)^{1/2} \qquad (2.3.6)$$

where $A=(\theta-\mathrm{Sin}(\theta))D^2/8$ is the flow area, with $\theta = 2\,\mathrm{Cos}^{-1}(1-2\Delta h/D)$. If the orifice/pipe opening is submerged, then an orifice flow equation is used (FHWA 1996):

$$Q = C_o\, A_o\, (2g\,(\Delta h - D/2.))^{1/2} \qquad (2.3.7)$$

where C_o= 0.55, A_o= $\pi D^2/4$, and the quantity (Δh - D/2) is the distance from the water surface to the centerline of the orifice. For pipe outflows, the maximum possible flow through a full pipe (Q_f) is calculated using Equation 2.3.8 (Mays 2001), and the outflow calculated using 2.3.6 or 2.3.7 is limited to the full pipe flow.

$$Q_f = (\pi D^2/4.0)(2g\,\Delta h_p/(1.+K_e+(20.0\,n^2\,L/(D/4.)^{1.33})))^{1/2} \qquad (2.3.8)$$

where K_e= 0.5, L is the pipe length, n is Manning's roughness coefficient, Δh_p is the difference in elevation between the two ends of the pipe. Equation 2.3.8 is also used to calculate the outflow for a submerged pipe case, as in Figure 2.3.2, lower panel. For ponds with multiple outlet types, e.g. an orifice and a weir, outflow contributions from the multiple outlets are calculated separately and added. To improve the accuracy and stability of the pond volume calculations, the outflow is calculated based on an estimated average stage (ST_{ave}) for the time step:

$$ST_{ave} = ST_o + (\Delta t/2)\, Q_{in}/A_{top} + (P - h_{evap} - h_{inf}) \qquad (2.3.9)$$

where ST_o is the stage at the beginning of the time step (Δt), Q_{in} is the total inflow rate, Atop is the surface area of the pond surface, and P, h_{ev}, and h_{in} are the precipitation, evaporation, and infiltration depths for the time step.

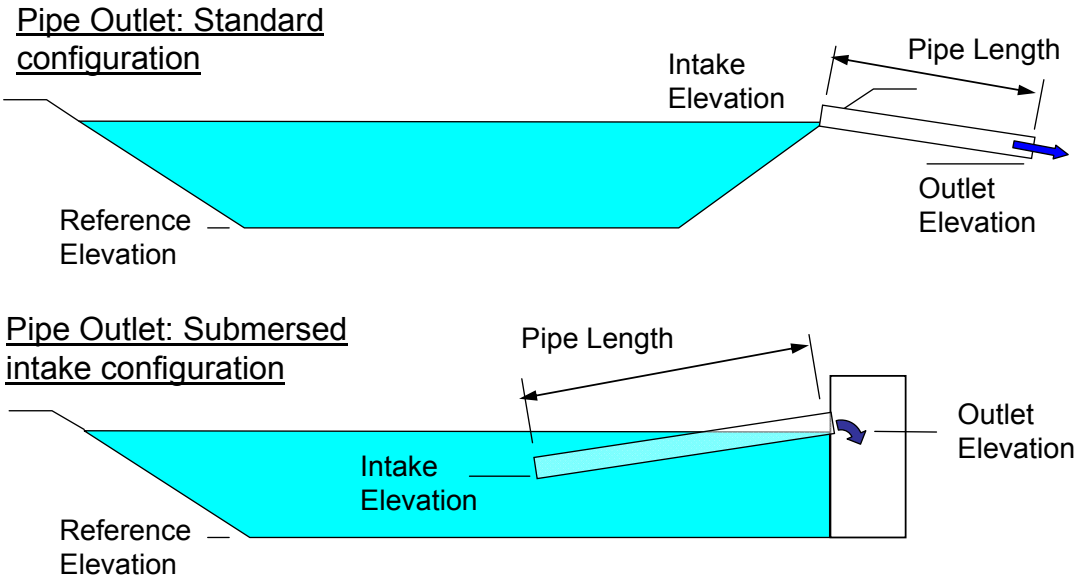

Figure 2.3.2. Schematic diagram of a wet pond with a pipe outlet in a standard configuration (top) and a submersed intake configuration (bottom).

Pond Water Temperature Model

The vertical temperature profile computations use the finite difference model developed for MINLAKE (Ford and Stefan 1980, Hondzo and Stefan 1993), as follows:

1. The 1-D (vertical) heat diffusion/conduction equation is solved for the composite water/sediment column.
2. Density instabilities in the water column are removed by a mixing algorithm.
3. The surface mixed layer depth and temperature are calculated using a surface wind mixing algorithm, and the temperature profile is adjusted.

The heat diffusion/convection model uses a calculated heat flux between the water surface and the atmosphere as an upper boundary condition, and a specified soil temperature as a lower boundary condition. The unsteady, 1-D heat conduction equation is

$$\frac{\partial T}{\partial t} = \frac{\partial}{\partial z}\left(D_z \frac{\partial T}{\partial z} \right) + \frac{S}{\rho C_p} \qquad (2.3.10)$$

where T is water temperature, t is time, z is vertical distance below the water surface, D_z is the vertical thermal diffusion coefficient in the pond, S is the heat source term, ρ is density, and C_p is specific heat. Equation 2.3.10 is applied to a composite of the water column and underlying soil by specifying appropriate values of the thermal diffusivity, density, and specific heat for each layer. The finite difference equation used to find each layer's temperature T_i is:

$$C_{i-1}T_{i-1,j+1} + C_iT_{i,j+1} + C_{i+1}T_{i+1,j+1} = C_oT_{i,j} + S_i \qquad (2.3.11)$$

with

$$C_{i-1} = -(2.0/(C_i \Delta z_i))\ A_{T,i}\ D_z/(\Delta z_i+\Delta z_{i-1}) \quad (2.3.12)$$
$$C_i = 1/\Delta t - C_{i-1} - C_{i+1} \quad (2.3.13)$$
$$C_{i+1} = -(2/V_i)\ A_{T,i+1} D_z(/(\Delta z_i+\Delta z_{i+1}) \quad (2.3.14)$$
$$C_o = 1/\Delta t \quad (2.3.15)$$

where $A_{T,I}$, V_i and Δz_i are the top area, volume and thickness of layer *i*, respectively, and Δt is the time step. Formulations for the hypolimnetic vertical diffusion coefficient (D_z) developed for lakes (Hondzo and Stefan 1993) were found to be inappropriate for a stormwater pond. Good results were obtained by setting D_z equal to molecular diffusion. The thermal diffusion model solves for water temperature and soil temperature to a depth of 10 m below the pond bottom. The lower boundary condition is a specified temperature based on mean annual air temperature (Fang and Stefan 1996). The source term S for the i^{th} water layer is calculated based on light attenuation in the water column:

$$S_i = (AT_i - AT_{i+1})\ I_i\ Exp(-K_T\ \Delta z_i)/V_i \quad (2.3.16)$$
$$I_i = I_{i-1} Exp(-K_T\ \Delta z_i) \quad (2.3.17)$$

where V_i is the layer volume, I_i is the incoming solar radiation for each layer, K_T is the total light attenuation coefficient.

Following the solution to the heat conduction equation, an algorithm checks for density instabilities, i.e. a more dense water layer above a less dense layer. Starting from the surface and proceeding down in the water column, if an unstable condition is found, the layers are mixed to create a volume-averaged temperature. This vertical mixing mechanism can be significant during nighttime surface cooling, and can result in complete mixing of the water column for shallow water bodies such as detention ponds.

Finally, the mixed layer depth is calculated for each time step based on a balance between kinetic energy from the wind and the potential energy of temperature stratification (Ford and Stefan 1980). The kinetic energy per unit area (KE) available for mixing is calculated from the surface shear stress (τ) and shear velocity (u*) using Equation 2.3.18:

$$KE = \tau \cdot \Delta t \cdot u^* \quad (2.3.18)$$

Surface shear stress and shear velocity are calculated based on wind speed and fetch using expressions given by Wu (1971). The potential energy of stratification for each layer is calculated as:

$$PE_i = g\, z_i \left(z_{i+1} - z_{cm}\right) \Delta\rho \quad (2.3.19)$$

where z_i is the mean depth of layer i, z_{cm} is the depth of the center of mass of the mixed layer, and $\Delta\rho$ is the density change from the mixed layer to layer *i*+1. Beginning at the surface and

working down, layers are incorporated into the mixed layer until the potential energy sum exceeds the kinetic energy.

The temperature of the outflow is calculated based on the vertical temperature profile of the pond and the depth of the outlet port below the pond surface, using an algorithm similar to that developed for the reservoir model RESQUAL II (Stefan et al. 1982). For a surface outlet, the withdrawal depth (z_w) is estimated based on Bernoulli's equation as:

$$z_w = \frac{\rho_w}{\rho_{zw} - \rho_w} \frac{V_w^2}{2g} \qquad (2.3.20)$$

where ρ_w is the density of the outflow, ρ_{zw} is the water density at z_w, V_w is the average outflow velocity, and g is the acceleration of gravity. The outlet temperature is then calculated as the water temperature averaged over the withdrawal depth.

For the event based analysis in MINUHET, appropriate temperature initial conditions must be set for the water and sediment layers. The sediment temperature distribution is set based on calendar day using empirical functions, using similar methods as those used for setting the soil temperature in the sub-watershed model. Two polynomial fits are used to estimate the pond surface temperature (T_s) and bottom temperature (T_b):

$$T_b = C_{T0} + C_{T1}\,Cday + C_{T2}\cdot\,Cday^2 + C_{T3}\,Cday^3 + C_{T4}\,Cday^4 \qquad (2.3.21)$$

$$T_s = C_{T10} + C_{T11}\,Cday + C_{T12}\cdot\,Cday^2 + C_{T13}\,Cday^3 + C_{T14}\,Cday^4 \qquad (2.3.22)$$

where Cday is the calendar day. The coefficients C_{T0}-C_{T4} and C_{T11}-C_{T14} were determined for the Twin Cities area from several years of simulated pond temperature data as:

C_{T0} = 72.89, C_{T1} = -1.799, C_{T2} = 1.625E-02, C_{T3} = -5.499E-05, C_{T4} = 6.123E-08

C_{T10} = 42.85, C_{T11} = -1.222, C_{T12} = 1.304E-02, C_{T13} = -4.853E-05, C_{T14} = 5.787E-08

Since actual seasonal pond temperatures vary with parameters such as depth and water clarity, a two week period of antecedent climate is used to initialize pond temperature prior to the storm event to be simulated. This two week period gives sufficient time for the pond temperatures to adjust to, e.g., the specific water clarity, depth and shading levels for the pond being modeled.

3. Model Application and Verification

Verification and calibration has been performed for the model components of MINUHET and for the coupled model. Although the implementation of the model components (sub-watershed

model, routing model, and pond model) in MINUHET is for event based analysis, versions of the sub-watershed and pond models have also been developed for continuous analysis. Analysis of, e.g., continuous land or water surface temperature time series gives very good evidence of the ability of model components to capture important heat transfer processes. Model verification studies have included comparisons of MINHUET simulation results to field data and comparisons to other well-established models such as EPA-SWMM.

Surface Temperature Model

The surface temperature component of the sub-watershed model has been verified and calibrated in 6 month continuous analysis for a number of different previous and impervious and uses, including pavement, rooftops, bare soil, grass, and crops (Herb et al. 2008b). For application to the MINUHET model, the most important verification is for wet weather surface temperatures. An example of such a temperature simulation is given in Figure 3.1 and 3.2, which gives the simulated and observed temperature time series and pavement/soil temperature profiles for an asphalt test section at the MnROAD facility in Albertville, MN during a precipitation event on August 16, 2005. The surface temperature model is capable of simulating pavement surface temperatures with an RMSE of 1 - 2ºC and pervious/vegetated surface temperatures with an RMSE of 1 - 3ºC. The roof temperature algorithm was also calibrated and verified for residential (shingle) and commercial (tar/gravel) roof surfaces, with RMSEs in the range of 2 - 3ºC. Further details may be found in Herb et al. 2008b.

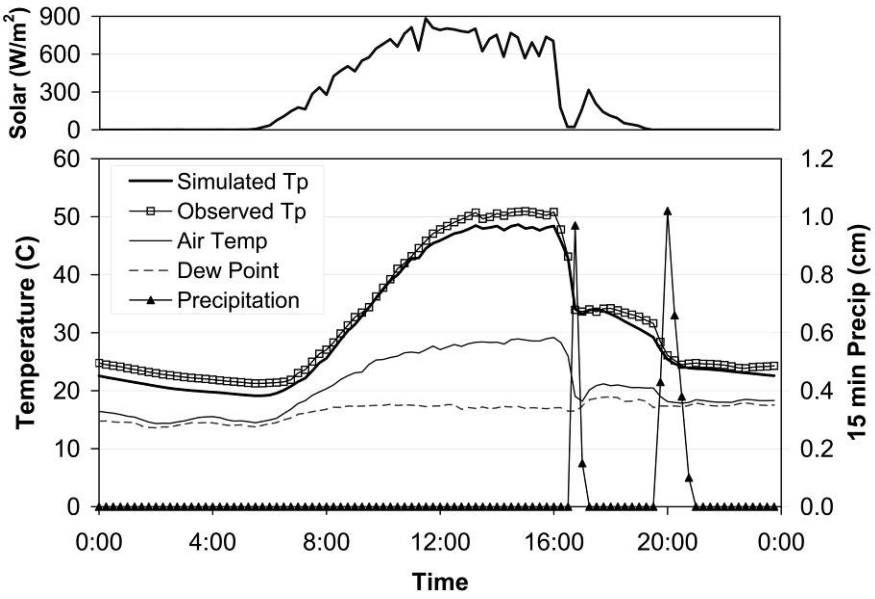

Figure 3.1. Time series plots of simulated and observed pavement temperature at 2.5 cm depth, observed air temperature, dew point temperature, and precipitation for August 16, 2005. All observed data are from the MnROAD facility in Albertville, MN.

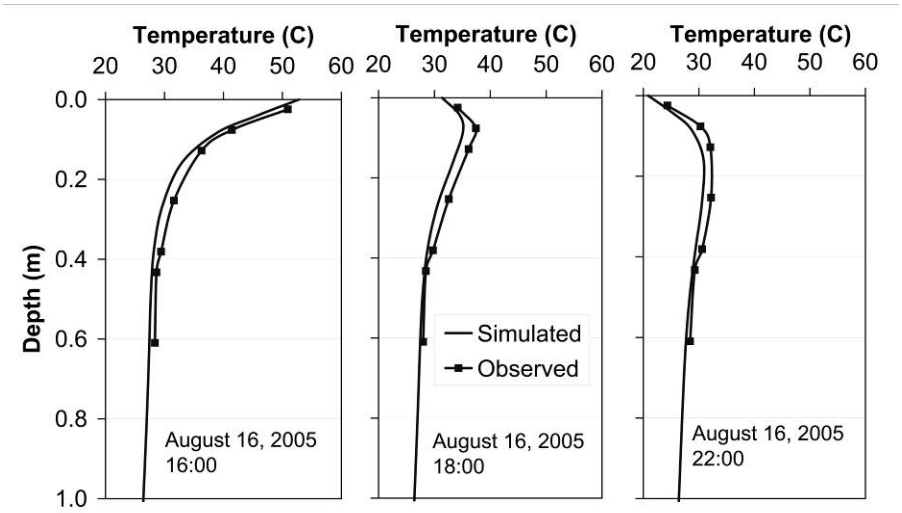

Figure 3.2. Observed and simulated ground temperature profiles for an asphalt test section and the underlying sub-grade and soil. Rainfall started at 16:00 hours. Observations are from the MnROAD facility in Albertville, MN on August 16, 2005.

Sub-watershed Model

The MINUHET sub-watershed runoff model has been compared to a kinematic wave model (Herb et al. 2006c), and the EPA-SWMM model. The runoff model has been found to mimic the response of a 1-D kinematic wave model for rainfall events with both steady and time-varying precipitation rates. An example comparison between simulation results for the MINUHET runoff model and for a kinematic wave model is given in Figure 3.3. Further comparisons are given in Herb et al. 2006c. In addition, a simple comparison analysis was made between MINUHET and EPA-SWMM, which uses a non-linear reservoir model for surface runoff (Huber and Dickinson 1988). For a 100% impervious surface, agreement between the MINUHET and EPA-SWMM results was reasonable, with very close agreement on the timing of the peak flow, and differences of peak flow magnitudes of less than 20% (Figure 3.4). For a 100% pervious surface (Figure 3.5), very good agreement between the MINUHET and EPA-SWMM was obtained for total runoff volume (within 1.5%) and peak flow rate (within 3%). Finally, the total runoff volume was calculated using both models for a range of pervious/impervious fractions and for a range of sub-catchment lengths (100 – 1500 m). This analysis was performed primarily to test the MINUHET infiltration algorithms at different runoff length scales. Again, agreement between the MINUHET and EPA-SWMM was quite good for a range of pervious/impervious fractions and length scales, indicating that the Green-Ampt infiltration algorithm used in MINUHET is performing as expected.

The coupled runoff rate and temperature model has been tested using field data from a commercial site in Woodbury, MN (Herb et al. 2008c), where both runoff flow rates and temperature were available for several months in 2005. The response of the 24 acre parking lot to three mid-summer rainfall events (July 2005) was simulated. The simulated and observed response to a storm on July 25, 2005 is shown in Figure 3.6. The model was found to predict the

average runoff temperatures within 0.5ºC of observed values, and total runoff volumes within 15%. The root-mean-square error of simulated runoff temperatures was 1.1 ºC.

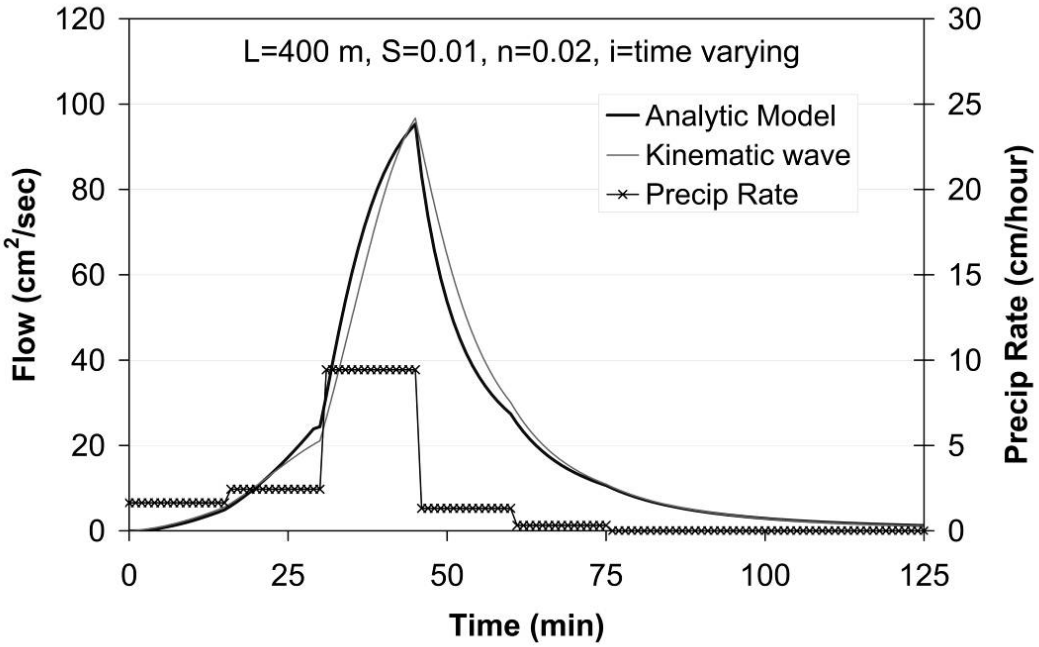

Figure 3.3. Simulated hydrographs for time-variable rainfall intensity for a 400m long impervious surface. The semi-analytic runoff model and the kinematic wave model were run at 60 s and 10 s time steps, respectively.

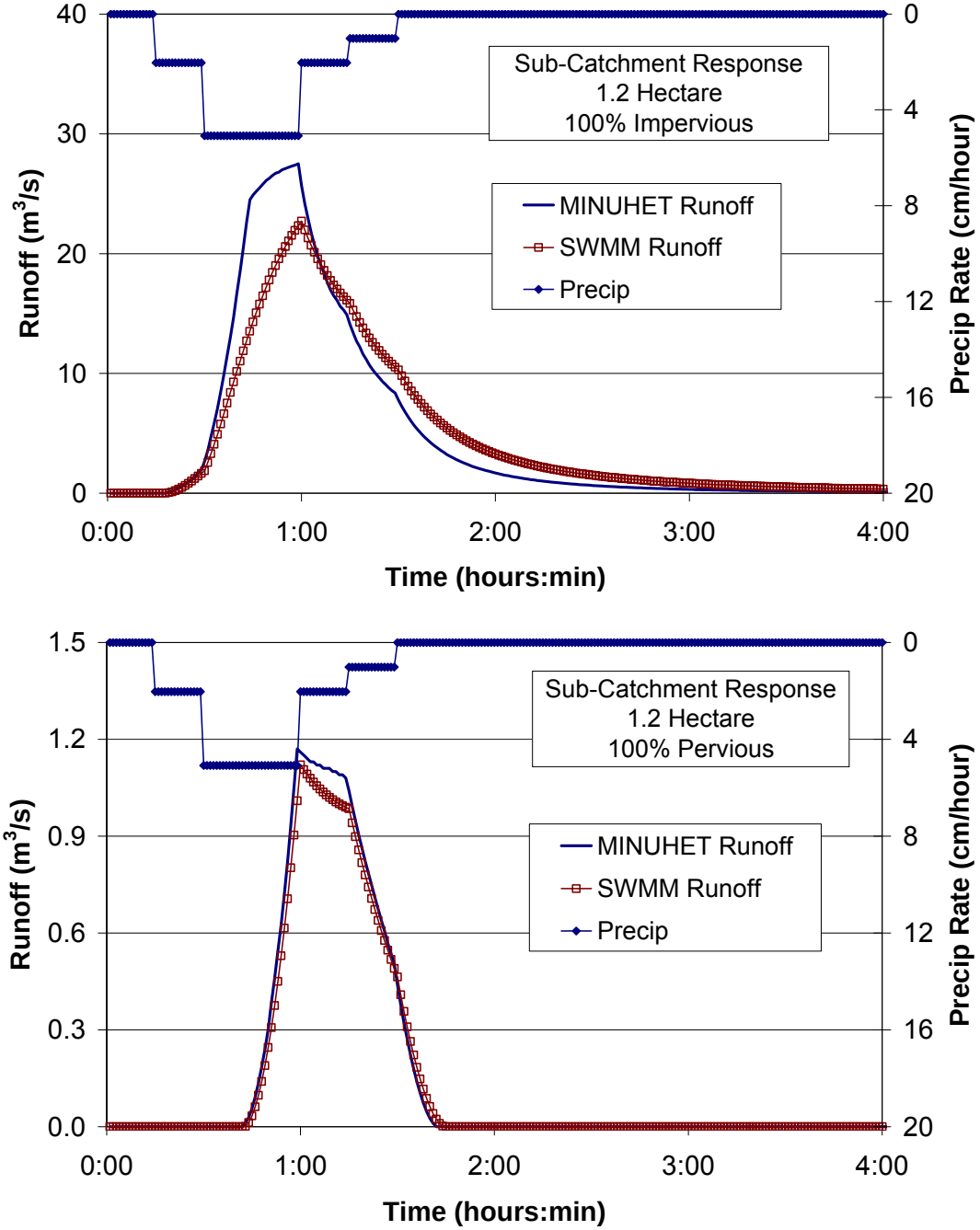

Figure 3.4. Runoff time series for analysis of a 100% impervious (upper panel) and 100% pervious (lower panel), 3 acre land area using MINUHET and EPA-SWMM. Runoff length = 110 meter, slope = 2%.

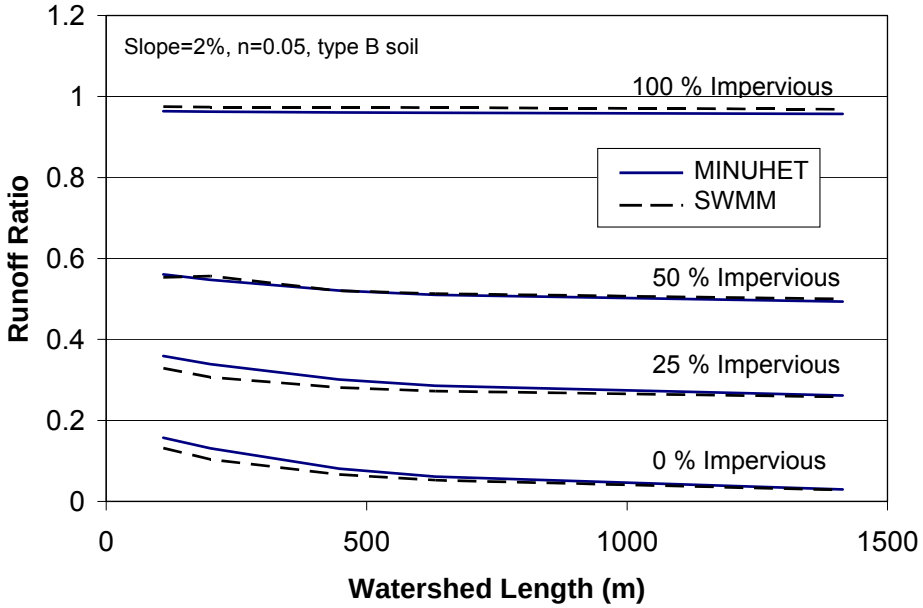

Figure 3.5. Runoff ration (runoff volume/precipitation volume) for analyses of land areas with different lengths and pervious/impervious fractions using MINUHET and EPA-SWMM.

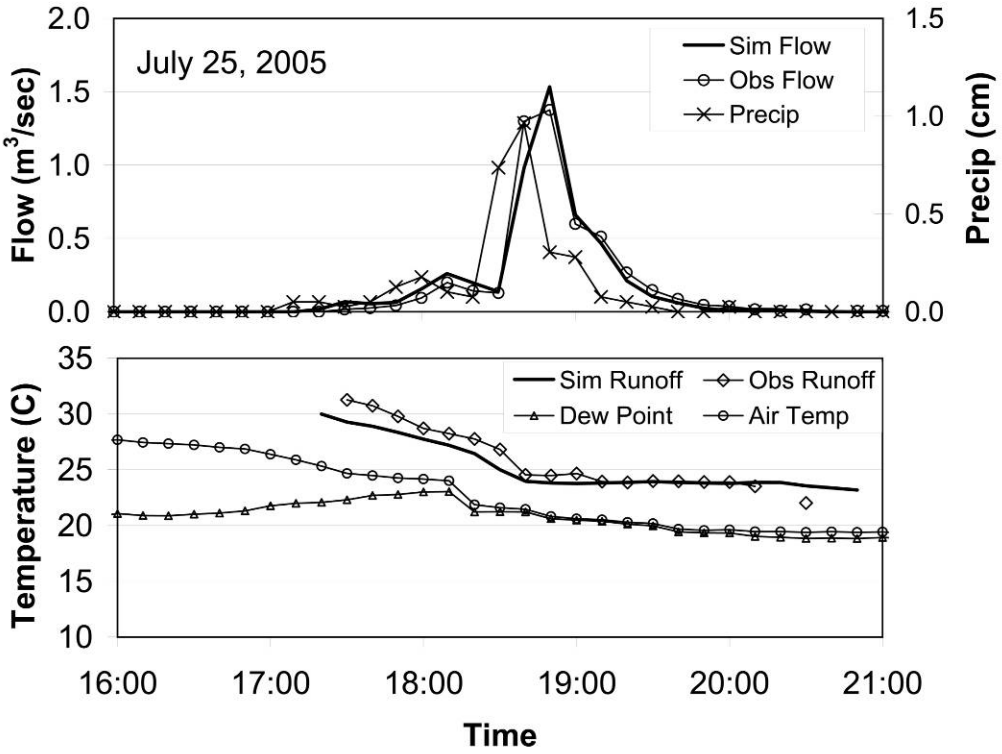

Figure 3.6. Simulated and observed runoff rate and temperature for runoff from a 24 acre parking lot in Woodbury, MN on July 25, 2005.

Pond Model

Data from a wet detention pond at the Woodbury, MN site were used to verify and calibrate the MINUHET pond model (SAFL Report #479, Herb et al. 2006b). The field data set included a partial climate station, a water level sensor, a thermistor string to measure the pond vertical temperature profile, and temperature loggers at the inlet and outlet. The pond model was found to predict pond outflow temperatures with an RMSE of 0.7ºC. An example of the simulated and predicted outlet temperature for the pond is given in Figure 3.7.

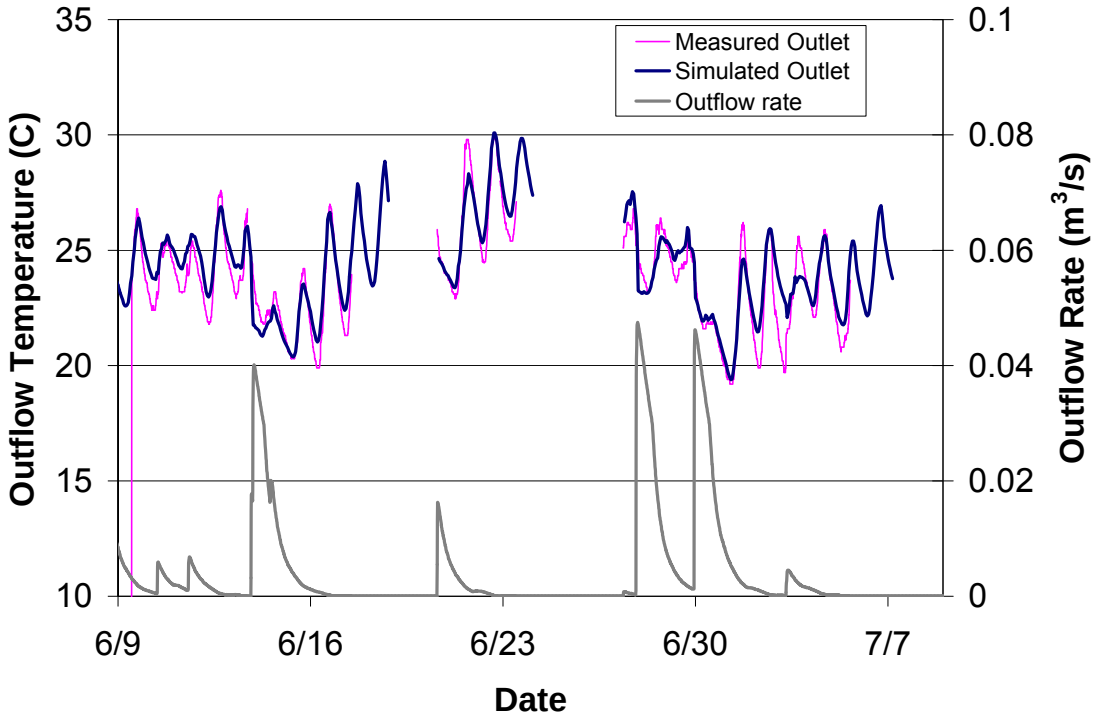

Figure 3.7. Simulated and observed pond outlet temperature and simulated pond outflow rate versus time, using the calibrated water clarity values. The outflow temperature is plotted only for time periods when the outflow rate is non-zero.

Coupled MINUHET Model

Several test cases have been studied to evaluate the ability of MINUHET to simulate runoff and runoff temperature from areas of mixed land use with a storm sewer network. MINUHET has been applied to a residential site in Plymouth, MN and a commercial site in Hastings, MN. For the residential site in Plymouth, observed runoff flow rates and temperatures were available for comparison to the MINUHET simulations for several rainfall events (Janke et al. 2007). The simulated runoff rates matched observed values quite well (Figure 3.8), while the simulated runoff temperatures differed from the observed temperatures by 1-2ºC (Figure 3.9), which was in part attributed to a lack of local dew point temperature measurements.

In addition, comparisons were made for the Plymouth residential site between runoff volume and peak flow rates for simulations using MINUHET and XP-SWMM (SAFL Report #520, Herb et

al. 2008a). For a 2.8" rainfall event (SCS Type II, 2 year, 24 hour storm), MINUHET was found to agree with SWMM within 1 to 14% for runoff volume and 4 to 40% for peak runoff flow rate (Table 3.1), including several hypothetical treatment pond configurations. No comparisons on runoff temperature were possible, since XP-SWMM does not consider temperature.

A second comparison of the MINUHET and XP-SWMM models was made for a commercial site in Hastings, MN (Herb et al. 2008a). The commercial site (Wal-mart) was modeled in some detail in MINUHET using 24 separate sub-watersheds and 25 pipe elements to model the land surfaces, roof areas, and drainage network. As with the Plymouth site, runoff from the site was simulated using both the MINUHET and EPA-SWMM models for an unmitigated case and for several cases with hypothetical rate and volume control ponds, including a low impact development (LID) case. MINUHET was found to agree with SWMM within 1 to 30% for runoff volume and 2 to 45% for peak runoff flow rate (Table 3.2).

Table 3.1. Comparison of runoff volume and peak runoff rate obtained with MINUHET and XP-SWMM (Barr Engineering, Wilson and Barnes 2008) for the Plymouth, MN residential site.

Case	Runoff Volume (acre-ft)		Peak Runoff Rate (cfs)	
	MINUHET	XP-SWMM	MINUHET	XP-SWMM
Undeveloped (Agricultural)	0.55	0.63	8.3	8.0
Developed, no mitigation	1.27	1.28	6.8	7.9
Developed, rate control only	1.31	1.24	6.2	5.8
Developed, rate and volume control	0.59	0.61	3.4	2.3

Table 3.2. Comparison of runoff volume and peak runoff rate obtained with MINUHET and XP-SWMM (Barr Engineering, Wilson and Barnes 2008) for the commercial development.

Case	Runoff Volume (acre-ft)		Peak Runoff Rate (cfs)	
	MINUHET	XP-SWMM	MINUHET	XP-SWMM
Undeveloped (Agricultural)	1.4	1.4	13.1	12.8
Developed, no mitigation	5.3	5.3	66.0	56.4
Developed, rate control only	5.2	3.8	13.4	10.7
Developed, rate and volume control	1.4	1.4	1.0	1.2
Developed, LID	1.2	1.2	0.7	1.1

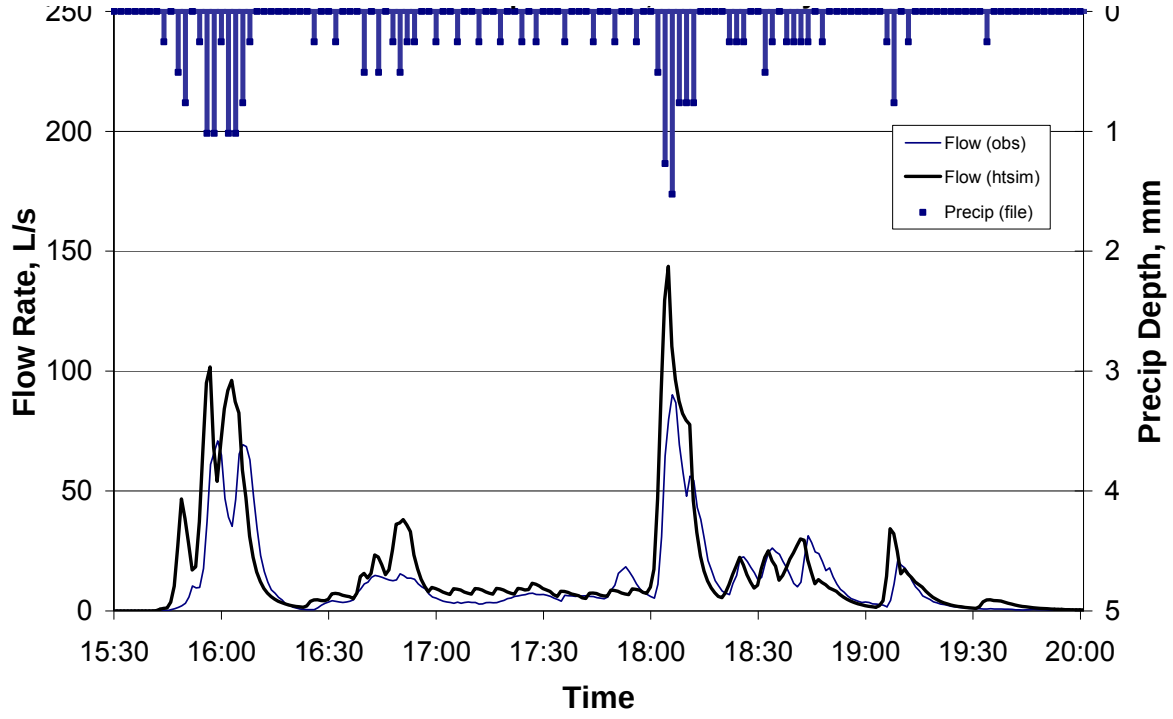

Figure 3.8. Observed and simulated hydrographs for a 2.3 cm rainfall event on September 3, 2005 at the Plymouth residential site.

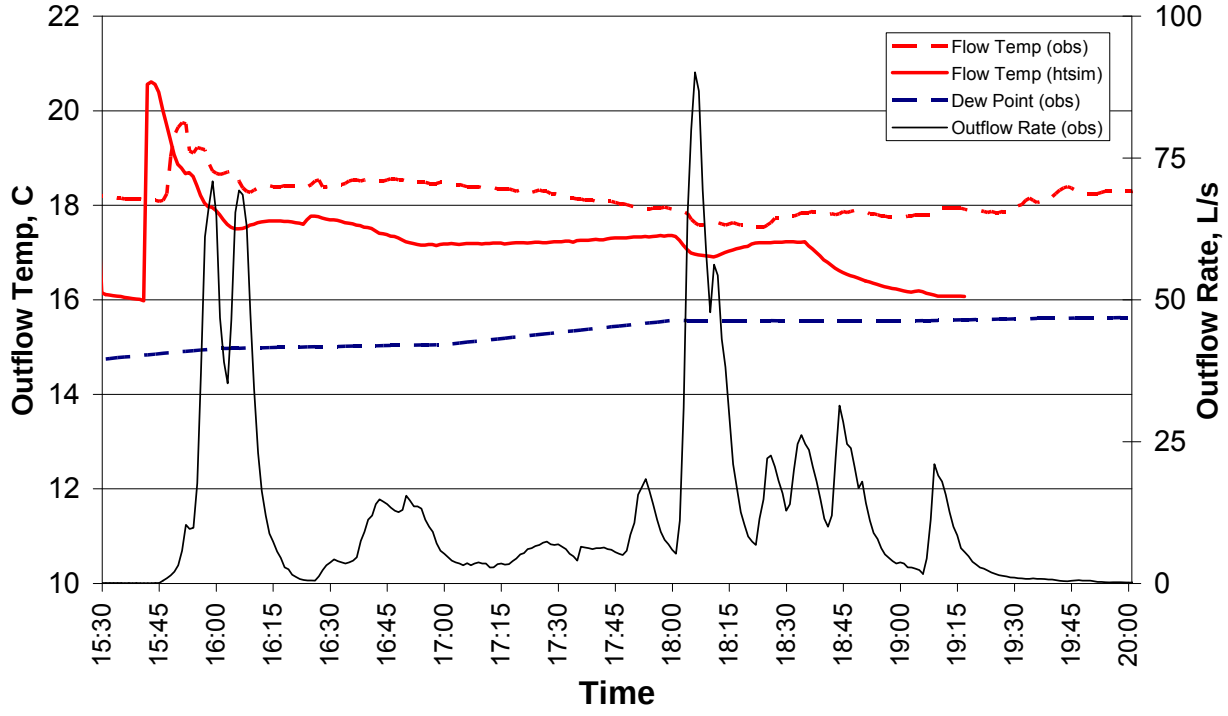

Figure 3.9. Observed runoff flow rate and runoff temperature and simulated runoff temperature for a 2.3 cm rainfall event on September 3, 2005 at the Plymouth residential site.

4. Conclusions

A new simulation tool, MINUHET (Minnesota Urban Heat Export Tool) has been created for simulating the flow of stormwater surface runoff and its associated heat content through a small watershed for one or several rainfall events. The main output of MINUHET is a time series of flow rates and temperatures at the outlet of the watershed, to enable prediction of thermal impact on receiving streams. MINUHET is a self-contained software tool that includes several model component FORTRAN 90 executables and a graphical user interface. MINUHET includes components for developed and undeveloped land parcels (sub-watersheds), pervious and impervious open channels, storm sewer systems, and stormwater ponds. The drainage network can include mitigation ponds, including wet ponds, dry ponds, infiltration ponds, and rain gardens.

Verification of MINUHET has been performed at both the component level and the system level. The surface temperature model was verified for a number of different impervious and pervious land surfaces for continuous, multi-month simulations of wet and dry conditions. The runoff model hydrologic component has been compared to other models, including a more complex kinematic wave model and a commercial runoff model (EPA-SWMM), and to observed runoff time series from a parking lot. The runoff temperature component was verified via comparisons to a more complex, 2-D model and using runoff time series from a parking lot. The MINUHET pond model component was used successfully to simulate several months of observed water level and temperature data for a wet detention pond in Woodbury, MN. The MINUHET tool has been applied to a 12 acre residential development in Plymouth, MN that was instrumented in 2005. The observed runoff hydrograph was successfully reproduced by MINUHET for several storm events. Predicted runoff temperatures differed from observed values by 1-2 ºC, mainly due to a lack of locally measured dewpoint temperature. More verification of MINUHET is needed for the storm sewer routing model and the surface runoff model for sub-watershed with mixed land use.

Acknowledgments

This study was conducted with support from the Minnesota Pollution Control Agency, St. Paul, Minnesota, with Bruce Wilson as the project officer. Runoff, soil temperature and climate data used in this study were supplied by
:

1) Dr. David Ruschy, University of Minnesota, Department of Soil, Climate and Water, made available the St. Paul soil and climate data.
2) Ben Worel and Tim Clyne, Minnesota Department of Transportation, made available climate and pavement temperature data from the MnROAD site.

3) Climate and soil temperature data was obtained for sites at Ames, Iowa and Mount Mansfield, Vermont from the Natural Resources Conservation Service Soil and Climate Analysis Network (http://www.wcc.nrcs.usda.gov/scan).
4) Climate and soil temperature data was obtained for sites at Bondville, Illinois from the Oak Ridge National Lab Ameriflux network (http://public.ornl.gov/ameriflux/). The PI responsible for this measurement site is Tilden Meyers NOAA/ARL, Atmospheric Turbulence and Diffusion Division.
5) Runoff data from several sites in Plymouth, MN used in this study were supplied by the Three Rivers Park District (James Johnson).
6) Surface and water temperature data from the Woodbury, MN site were collected by Michael Weiss (St. Anthony Falls Lab).

Additional funding for MINUHET applications was provided by The Vermillion River Watershed Joint Powers Organization, with Paul Nelson as project officer. Barr Engineering Co. supplied plans and land use data for the Wal-Mart site, treatment pond designs for both the residential and commercial sites, and XP-SWMM simulation results that were obtained in a separate study.

We are grateful to these individuals and organizations for their cooperation.

References

Chow, V.T. (1964). *Handbook of Applied Hydrology.* McGraw-Hill Inc., New York, NY.

Eckert, E.R.G., and R.M. Drake (1972), *Analysis of Heat and Mass Transfer*, McGraw-Hill.

Fang, X. and H.G. Stefan (2000). Dependence of Dilution of a Plunging, Submerged Discharge Over a Sloping Bottom on Inflow and Bottom Friction, *Jour. of Hydraulic Research,* 38(1): 15-26.

Federal Highway Administration (FHWA) (1996), Urban Drainage Manual, HydraulicEngineering Circular No.22, FHWA-SA-96-078, Washington D.C.

Ford, D.E. and H.G.Stefan (1980). Thermal prediction using integral energy model. *J. Hydraulics Division* ASCE 106(1): 39 -55.

Gu, R. and H.G. Stefan (1995). Stratification dynamics in wastewater stabilization pond. *Water Research* 29(8): 1909 – 1923.

Herb, W.R, B. Janke, O. Mohseni and H.G. Stefan (2006a). All-Weather Ground Surface Temperature Simulation. Project Report No. 478, St. Anthony Falls Laboratory, University of Minnesota, September 2006, 57pp.

Herb, W.R, M. Weiss, O. Mohseni and H.G. Stefan (2006b). Hydrothermal Simulation of a Stormwater Detention Pond or Infiltration Basin. Project Report No. 479, St. Anthony Falls Laboratory, University of Minnesota, September 2006, 35pp.

Herb, W.R, B. Janke, O. Mohseni and H.G. Stefan (2006c). Analytic Model for Runoff and Runoff Temperature from a Paved Surface. Project Report No 484, St. Anthony Falls Laboratory, University of Minnesota.

Herb, W.R (2008a). Analysis of the effect of stormwater runoff volume regulations on thermal loading to the Vermillion River. Project Report No 520, St. Anthony Falls Laboratory, University of Minnesota.

Herb, W.R., B. Janke, O. Mohseni and H.G. Stefan, (2008b). Ground surface temperature simulation for different land covers, *J. Hydrology*, 356(3): 327-343.

Herb, W.R., B. Janke, O.Mohseni, and H. G. Stefan (2008c). A model for runoff and thermal pollution from paved surfaces, In revision, *J. Hydrologic Engineering*.

Hondzo, M. and H. G. Stefan (1993). Lake Water Temperature Simulation Model, Jour. of Hydraulic Engineering, ASCE, 119(11), 1251-1273.

Huber, W. C. and Dickinson, R. E. (1988). *Stormwater Management Model, Version 4 Part A: User's Manual.* Rep. No. EPA/600/3-88/001a, U.S. Environmental Protection Agency, Athens, GA.

Janke, B., W.R. Herb, O. Mohseni and H.G. Stefan, (2007). Application of a Runoff Temperature Model (MINUHET) to a Residential Development in Plymouth, MN. Project Report No 497, St. Anthony Falls Laboratory, University of Minnesota, 34pp.

Li, R. M., Stevens, M. A., and Simons, D. B. (1976). "Solutions to Green-Ampt infiltration equation." J. Irrig. and Drain. Div., ASCE, **102**(2), 239–248.

Mays, L.W. (2001). *Water Resources Engineering,* First Ed., John Wiley and Sons, New York.

Ochsner, T.E., Horton, R., and Ren, T. 2001. A new perspective on soil thermal properties. Soil Sci. Soc. Am. J., 65: 1641-1647.

Stefan, H. G., Cardoni, J. J., and A.Y. Fu (1982). RESQUAL II: A dynamic water quality simulation program for a stratified shallow lake or reservoir: Application to Lake Chicot, Arkansas. Project Report 209, University of Minnesota, St. Anthony Falls Hydraulic Laboratory 146p.

Wilson, G. and Barnes, B., 2008. VRWJPO Runoff Volume Standard Analysis: Methodology and Results. Technical Memorandum, Barr Engineering Co.

Wu, J. (1971). Anemometer height in Froude scaling of wind stress. *J. Waterway, Harbor, Coastal Engineering Division* ASCE 98(WW1): 131-137. Proc. Paper 7873.

Appendix A: Surface Heat Transfer Formulation for Bare Surfaces

The model for net surface heat flux (h_{net}) for bare surfaces such as pavement, rooftops, and bare soil considers the surface properties (roughness, albedo, and emissivity) and the weather conditions (e.g. solar irradiance, air temperature, wind speed, relative humidity or dew point temperature) to calculate net radiation (h_{rad}), evaporation (h_{evap}), and convection (h_{conv}) heat fluxes from the land surface to the atmosphere (Equations A.1 - A.8)

The evaporative heat transfer formulation (Equation A.3) uses the aerodynamic method at hourly or shorter time steps. The evaporation and convection heat transfer components consider both forced convection, proportional to wind speed, and natural convection, related to the difference in temperature between the surface and the atmosphere. For paved surfaces, the evaporative heat flux is calculated only when standing water is present, either during runoff or due to depressional storage. The wind velocity at 10m height (u_{10}) is scaled by a sheltering coefficient (CS_h) to take into account the effect of trees, buildings, and topographical features on surface wind velocity (u_s).

$$h_{net} = h_{rad} - h_{evap} - h_{conv} - h_{ro} \quad (A.1)$$

$$h_{rad} = h_s + h_{li} - h_{lo} \quad (A.2)$$

$$h_{evap} = \rho_a L_v \left(C_{fc} u_s + C_{nc} \Delta\theta_v^{0.33}\right)\left(q_{sat} - q_a\right) \quad (A.3)$$

$$h_{conv} = \rho_a c_p \left(C_{fc} u_s + C_{nc} \Delta\theta_v^{0.33}\right)\left(T_s - T_a\right) \quad (A.4)$$

$$h_s = \left(1 - \alpha_s\right) R_s \quad (A.5)$$

$$h_{li} = \varepsilon\sigma\left(CR + 0.67 \cdot \left(1 - CR\right) e_a^{0.08}\right) T_{ak}^4 \quad (A.6)$$

$$h_{lo} = \varepsilon\sigma T_{sk}^4 \quad (A.7)$$

$$u_s = CS_h\, u_{10} \quad (A.8)$$

where h_{ro} are the heat fluxes due to total net radiation, evaporation, and convection, respectively, and h_s, h_{li}, h_{lo}, and h_{ro} are the net solar, incoming long wave, outgoing long wave radiation, and surface runoff terms, respectively. ρ_a is the density of air, c_p and L_v are the specific heat and latent heat of vaporization of water, C_{fc} and C_{nc} are coefficients for forced and natural convection, respectively, $\Delta\theta_v$ is the difference in virtual temperature between the surface and atmosphere, q_{sat} and q_a are the saturated and ambient specific humidity, e_a is the ambient vapor pressure, α_s is the surface albedo, R_s is the incident solar radiation, T_s and T_a are the surface and air temperature in ^oC, T_{sk} and T_{ak} are the surface and air temperature in ^oK, ε and σ are the

surface emissivity and the Stefan-Boltzmann constant, respectively, and CR is the cloud cover ratio (0=full sun, 1=full cloud cover).

A novel feature of the heat transfer formulation is inclusion of conductive heat transfer between the ground (pavement) and the runoff. Heat input from precipitation is estimated based on the temperature difference between the precipitation and the runoff temperature at any time. The heat transfer model assumes (1) the precipitation is at dew point temperature, and (2) the runoff and the ground surface itself must equilibrate to the same temperature over the time step (Δt). To achieve this equilibrium, a conductive heat flux (h_{ro}) can be calculated which draws heat out of a thin layer of pavement with thickness, δ, at the ground surface. The thickness (δ) is estimated from the thermal properties of the pavement and the length of the time step (Δt), based on analytic solutions for heat conduction into an infinite slab subject to a change in surface temperature (Eckert and Drake, 1972):

$$\delta = \sqrt{4 D \Delta t} \qquad \text{(A.9)}$$

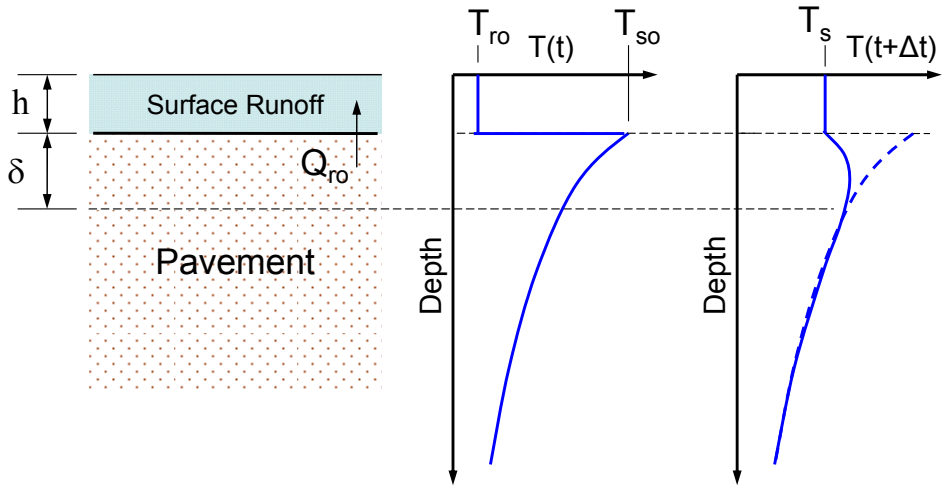

Figure A.1. Schematic of the formulation for heat transfer between surface runoff and the underlying pavement. Example temperature profiles show the temperatures in the pavement prior to a rainfall event (T(t)) and after a rainfall event (T(t+Δt)), where the initial surface temperature (T_{so}) has equilibrated with the initial runoff temperature (T_{ro}) to yield the new surface and runoff temperature (T_s).

For a time step of 15 minutes and a thermal diffusivity of 4 x 10^{-6} m^2/s, δ= 12 cm. An equation for the heat flux between the water layer on the runoff surface and the ground is written as:

$$h_{ro} = i\left(\rho c_p\right)_w \left(T_s - T_{dp}\right) = -\frac{\delta}{2\Delta t}\left(\rho c_p\right)_p \left(T_s - T_{so}\right) \ \text{(J/m}^2\text{)} \qquad \text{(A.10)}$$

where i is the precipitation rate, $(\rho c_p)_p$ and $(\rho c_p)_w$ are (density · specific heat) for the pavement and water, respectively, and the factor (δ/2) takes into account that the temperature change in the

pavement decreases with depth, whereas the temperature change in the water layer is (assumed to be) uniform across the thickness, *y*.

If other atmospheric heat transfer components were absent, Equation 2.1.14 could be directly solved for surface temperature. In this case, the runoff heat transfer is just one of several heat transfer components that determine surface temperature. In MINUHET, the surface temperature at the beginning of each time step (T_{so}) is used to estimate the conductive heat flux for each time step:

$$h_{ro} = i\left(\rho c_p\right)_w \left(T_{so} - T_{dp}\right)\left(\frac{\beta}{1+\beta}\right);\ \beta = \frac{\delta\left(\rho c_p\right)_p}{2P\left(\rho c_p\right)_w} \qquad \text{(A.11)}$$

where i is the precipitation rate and P is the rainfall depth for the time step. Using Equation A.11, the heat flux from the ground to the water layer (runoff) is estimated for each time step based on the precipitation rate, and is added to the atmospheric heat flux components.

The surface heat transfer equations given here are non-linear, e.g. the back radiation term (Equation A.7) depends on surface temperature to the 4th power. This non-linearity can lead to instability in the solution for surface temperature. To improve stability, it is helpful to linearize the surface heat transfer equations:

$$h_{net}\left(T_s\right) = h_{net}\left(T_{so}\right) + \frac{\partial h_{net}}{\partial T_s}\left(T_{so}\right)\left(T_s - T_{so}\right) \qquad \text{(A.12)}$$

where T_{so} is the known surface temperature from the previous time step and T_s is the unknown surface temperature for the current time step. The derivative $\partial h_{net}/\partial Ts$ can be evaluated at T_{so} using the following equations:

$$\frac{\partial h_{ne}}{\partial T_s} = \frac{\partial h_{lo}}{\partial T_s} + \frac{\partial h_{conv}}{\partial T_s} + \frac{\partial h_{evap}}{\partial T_s} \qquad \text{(A.13)}$$

$$\frac{\partial h_{lo}}{\partial T_s} = 4\varepsilon\sigma T_{sk}^3 \qquad \text{(A.14)}$$

$$\frac{\partial h_{conv}}{T_s} = \rho_a c_p \left(C_{fc} u_s + C_{nc} \Delta\theta_v{}^{0.33}\right) \qquad \text{(A.15)}$$

$$\frac{h_{evap}}{\partial T_s} = \rho_a L_v \left(C_{fc} u_s + C_{nc} \Delta\theta_v{}^{0.33}\right)\frac{\partial q_{sat}}{\partial T_s} \qquad \text{(A.16)}$$

Appendix B: Surface Heat Transfer Formulation for Vegetated Surfaces

The heat flux components considered in the plant canopy model are given by Equation B.1. It is assumed that the canopy has negligible heat capacity, so that heat flux components exactly balance each other during each time step. Expressions for the heat flux components are given in Equations B.2 – B.5. The net atmospheric radiation, $h_{rad,a}$, includes incoming long wave radiation, h_{li}, previously given by Equation 9. Note that all heat flux components are scaled by the vegetation density, ν, which varies from 0 to 1, where $\nu = 1$ corresponds to a leaf area index of approximately 7 (Deardorff, 1978):

$$h_{rad,a} - h_{rad,g} - h_{evap,f} - h_{conv,f} = 0 \tag{B.1}$$

$$h_{rad,a} = (1-\alpha_f)\nu R_s + \nu h_{li} - \nu \varepsilon_f \sigma T_{fk}^{\ 4} \tag{B.2}$$

$$h_{li} = \varepsilon\sigma\left(CR + 0.67 \cdot (1-CR) e_a^{\ 0.08}\right) T_{ak}^4 \tag{B.3}$$

$$h_{rad,g} = \nu \varepsilon_f \sigma T_{fk}^{\ 4} - \nu \varepsilon_g \sigma T_{sk}^{\ 4} \tag{B.4}$$

$$h_{evap,f} = \rho_a L_v \ \nu (q_{sat}(T_f) - q_a)/(r_a + r_s) \tag{B.5}$$

$$h_{conv,f} = \rho_a c_p \nu (T_f - T_a)/r_a \tag{B.6}$$

where $h_{rad,g}$, is the net radiative flux between the canopy and the ground, $h_{evap,f}$ and $h_{conv,f}$ are the canopy evaporative and convective heat fluxes, α_f is canopy albedo, ε_f and ε_g are the canopy and ground emissivity, T_f and T_{fk} are the canopy temperature in (°C) and (°K), q_a and q_{sat} are the ambient and saturated specific humidity. The aerodynamic (r_a) and stomata (r_s) resistance coefficients are calculated using expressions similar to those of Deardorff (1978):

$$r_a = 1/(c_f u_s) \tag{B.7}$$

$$c_f = 0.01(1 + 0.3/u_s) \tag{B.8}$$

$$r_s = 200\left(R_{s,max}/(R_s + 0.03 R_{s,max}) + (\theta_{wp}/\theta)^2\right) \tag{B.9}$$

where c_f is a transfer coefficient and $R_{s,max}$ is the maximum solar radiation.
The formulation for the ground surface heat flux is similar to those used for bare soil and pavements, except that the heat flux components are reduced as the canopy density is increased. The constant C_e establishes the level of soil evaporation for fully dense canopies, e.g. setting $C_e < 1$ gives non-zero soil evaporation for the full canopy case. The heat balance for the ground surface is given by Equation 29, and the heat flux components are specified by Equations 30 to 32:

$$h_{net,g} = h_{rad,net,g} - h_{evap,g} - h_{conv,g} - h_{ro} \tag{B.10}$$

$$h_{rad,net,g} = (1-\alpha_g)(1-\nu)R_s + (1-\nu)h_{li} + \nu \varepsilon_f \sigma T_{fk}^4 - \varepsilon_g \sigma T_{sk}^4 \tag{B.11}$$

$$h_{conv,g} = \rho_a c_p (1 - C_e \nu)\left(C_{fc} u_s + C_{nc} \Delta\theta_v^{\ 0.33}\right)(T_s - T_a) \tag{B.12}$$

$$h_{evap,g} = \rho_a L_v \theta' \left(1 - C_e \nu\right)\left(C_{fc} u_s + C_{nc} \Delta\theta_v^{0.33}\right)\left(q_{sat}(T_s) - q_a\right) \qquad (B.13)$$

where $h_{rad,net,g}$, $h_{conv,g}$ and $h_{evap,g}$ are the net radiative, convective, and evaporative heat flux at the ground surface, respectively, and α_g is ground albedo. To calculate the surface heat flux for each time step, Equations 21 to 28 are used to find a canopy temperature, based on values of air temperature, solar radiation, dew point, and wind speed. Since Equation 23 is non-linear in canopy temperature (T_f), it is solved using Newton's method. The calculated canopy temperature is then used to calculate the ground surface heat flux and its components using Equations 29 to 32. The soil evaporation and canopy evaporation are used to update the soil moisture content. Canopy interception is not included in the water budget analysis.

Appendix C. Surface Runoff Model Formulation

The runoff model is based on Manning's equation (C.1), which gives a relationship between runoff depth (y) and flow rate per unit width (q) for a land surface with a slope (S_0) and a Manning's roughness (n):

$$q = \frac{S_0^{1/2} y^{5/3}}{n} \qquad (C.1)$$

The runoff surface (of length, L) is divided into two regions: a length (L_e) with fully-developed (steady-state or equilibrium) flow where water depth (y) is variable with distance, and a length (L-L_e) of constant runoff depth (y). The time (t_e) required for the flow to reach equilibrium (steady-state) on a surface of length L, can be estimated from Equation (C.2) as (Mays 2001):

$$t_e = \frac{n L}{S_0^{1/2} y_L^{2/3}} \qquad (C.2)$$

where y_L is the flow depth at x=L. For excess rainfall intensity i, the equilibrium (steady-state) flow rate, q, at any distance, x, can be determined from a mass balance as:

$$q = i \cdot x \qquad (C.3)$$

Equations C.1 and C.3 can be combined to yield Equation (C.4) for y(x) at steady state flow:

$$y(x) = \left(\frac{i x n}{S_0^{1/2}}\right)^{3/5} \qquad (C.4)$$

By definition, Equation C.4 is applicable only over the region $0 < x < L_e$. Combining Equation C.2 with Equation C.4 at x = L yields an estimate for the time to equilibrium for the total length (L):

$$t_e = \left(\frac{n L}{i^{2/3} S_0^{1/2}}\right)^{3/5} \qquad (C.5)$$

For $t < t_e$, the runoff is equilibrated over a length L_e, where $L_e < L$. An expression for L_e as a function of time (t) may be found by rearranging Equation C.5:

$$L_e = \frac{S_0^{1/2} i^{2/3} t^{5/3}}{n} \tag{C.6}$$

The volume of water on the pavement per unit width (v) may be expressed as:

$$v = \frac{5}{8} h L_e + y(L - L_e) = y\left(L - \frac{3}{8} L_e\right) \tag{C.7}$$

where y = h at $x = L_e$. The time rate of change of the runoff volume on the pavement can be expressed in difference form as:

$$v(t + \Delta t) = v(t) + i L \Delta t - \frac{\Delta t}{2}\left(q_L(t) + q_L(t + \Delta t)\right) \tag{C.8}$$

where $q_L(t)$ is the runoff rate at the end of the pavement at time t. Using Manning's equation and Equation C.7, the water volume on the pavement can be expressed in terms of the flow rate as

$$v(t + \Delta t) = q_L(t + \Delta t)^{3/5}\left(\frac{n}{\sqrt{S_0}}\right)^{3/5}\left(L - \frac{3}{8} L_e(t + \Delta t)\right) \tag{C.9}$$

Substituting Equation C.9 into Equation C.8 gives

$$q_L(t + \Delta t)^{3/5}\left(\frac{n}{\sqrt{S_0}}\right)^{3/5}\left(L - \frac{3}{8} L_e(t + \Delta t)\right) + q_L(t + \Delta t)\frac{\Delta t}{2} = v(t) + i L \Delta t - q_L(t)\frac{\Delta t}{2} \tag{C.10}$$

Equation C.11 is non-linear in the unknown flow rate, $q_L(t+\Delta t)$. To linearize the equation, the following Taylor series expansion is used:

$$q_L(t + \Delta t)^{3/5} \approx q_L(t)^{3/5} + \frac{3}{5} q_L(t)^{-2/5}\left(q_L(t + \Delta t) - q_L(t)\right) \tag{C.11}$$

Substituting Equation C.11 into C.10 yields a linear difference equation for the new flow rate, $q_L(t+\Delta t)$ as a function of the previous flow rate,

$$q_L(t): q_L(t+\Delta t) = \frac{v(t) + i\,L\,\Delta t - q_L(t)\frac{\Delta t}{2} - \frac{2}{5}\left(\frac{n}{\sqrt{S_0}}\right)^{3/5}\left(L - \frac{3}{8}L_e(t+\Delta t)\right) q_L(t)^{3/5}}{\frac{\Delta t}{2} + \frac{3}{5}\left(\frac{n}{\sqrt{S_0}}\right)^{3/5}\left(L - \frac{3}{8}L_e(t+\Delta t)\right) q_L(t)^{-2/5}} \quad \text{(C.12)}$$

Based on the foregoing equations, the analysis of a rainfall event with constant intensity may proceed as follows:

1) For the first time step of the rainfall event, the water volume on the surface is estimated as $v(0) = i \cdot L \cdot \Delta t$, and the runoff depth as $y = i \cdot \Delta t$. The flow rate $q_L(\Delta t)$ at the end of the first time step is calculated using Manning's equation (Equation C.1).

2) For each subsequent time step during the rainfall event, Equation C.6 is used to calculate the equilibrated runoff length $L_e(t+\Delta t)$. Equation C.12 is used to calculate the runoff rate $q_L(t+\Delta t)$, and Equation C.8 is used to calculate the new water volume $v(t+\Delta t)$. L_e increases over time, but is not allowed to exceed L.
3) At the end of the rainfall event, the calculation continues with i=0 in Equation C.12. If L_e is less than L, i.e. the rainfall event is shorter than the time to equilibrium (steady-state for the entire runoff surface), L_e is assumed to follow Equation 7 as if the rainfall continues at the same intensity, and the entire length L stays wetted as the runoff thickness approaches zero.

For rainfall events with time varying intensity, Equation C.6 does not strictly apply, since its derivation assumes constant rainfall intensity. The application of a step discontinuity in rainfall intensity to Equation C.6 results in a discontinuous value of L_e and of the runoff volume. To eliminate this discontinuity, rainfall intensity in Equation C.6 is replaced by the running-average rainfall intensity (i_{ave}):

$$i_{ave}(t_1) = \frac{1}{t_1}\int_0^{t_1} i(t)\,dt \quad \text{(C.13)}$$